의학박사 학위논문

Role of Li^+-permeable Na^+/Ca^{2+} exchanger, NCLX, in the regulation of cytosolic Ca^{2+} and exocytosis in pancreatic β-cell

췌장 베타세포의 세포내 칼슘과 인슐린 분비 조절에 대한 리튬 투과성 소디움/칼슘 교환 기전의 역할

2015 년 8 월

서울대학교 대학원

의과학과 생리학 전공

한 영 은

A thesis of the Degree of Doctor of Philosophy

췌장 베타세포의 세포내 칼슘과 인슐린 분비 조절에 대한 리튬 투과성 소디움/칼슘 교환 기전의 역할

Role of Li^+-permeable Na^+/Ca^{2+} exchanger, NCLX, in the regulation of cytosolic Ca^{2+} and exocytosis in pancreatic β-cell

August 2015

The Department of Physiology,

Seoul National University

College of Medicine

Young Eun Han

췌장 베타세포의 세포내 칼슘과 인슐린 분비 조절에 대한 리튬 투과성 소디움/칼슘 교환 기전의 역할

지도 교수 호 원 경

이 논문을 의학박사 학위논문으로 제출함

2015 년 4월

서울대학교 대학원

의과학과 생리학 전공

한 영 은

한영은의 의학박사 학위논문을 인준함

2015 년 6 월

위 원 장 _____ (인)

부위원장 _____ (인)

위 원 _____ (인)

위 원 _____ (인)

위 원 _____ (인)

Role of Li^+-permeable Na^+/Ca^{2+} exchanger, NCLX, in the regulation of cytosolic Ca^{2+} and exocytosis in pancreatic β-cell

by

Young Eun Han

A thesis submitted to the Department of Physiology in partial fulfillment of the requirements for the Degree of Doctor of Philosophy in Physiology at Seoul National University College of Medicine

June 2015

Approved by thesis committee:

Professor _____ **Chairman**

Professor _____ **Vice chairman**

Professor _____

Professor _____

Professor _____

ABSTRACT

Na^+/Ca^{2+} exchangers are key players for Ca^{2+} clearance in pancreatic β-cells, but their molecular determinants and exact roles in insulin secretion are not fully understood. In the present study, I investigated the role of Na^+/Ca^{2+} exchangers on cytosolic Ca^{2+} dynamics and exocytosis in rat INS-1 insulinoma cells. I newly discovered that the Li^+-permeable Na^+/Ca^{2+} exchanger (NCLX), which is known as mitochondrial Na^+/Ca^{2+} exchanger, contributed to the Na^+-dependent Ca^{2+} movement across the plasma membrane in INS-1 cells. Na^+/Ca^{2+} exchange activity by NCLX was comparable to that by the Na^+/Ca^{2+} exchanger, NCX. I also confirmed the presence of NCLX proteins on the plasma membrane using immunocytochemistry and cell surface biotinylation experiments. I further investigated the role of NCLX on exocytosis function by measuring the capacitance increase in response to repetitive depolarization in small interfering (si)NCLX-transfected INS-1 cells. siRNA-mediated downregulation of NCLX did not affect the initial exocytosis, but significantly suppressed sustained exocytosis and recovery of exocytosis. XIP (NCX inhibitory peptide) or Na^+ replacement for inhibiting Na^+-dependent Ca^{2+} clearance also selectively suppressed sustained exocytosis. Consistent with the

idea that sustained exocytosis requires ATP dependent-vesicle recruitment, mitochondrial function, assessed by mitochondrial membrane potential ($\Delta\Psi$), was impaired by siNCLX or XIP. However, depolarization-induced exocytosis was hardly affected by changes in intracellular Na^+ concentration, suggesting a negligible contribution of mitochondrial Na^+/Ca^{2+} exchanger. In addition, I discovered that oligomycin inhibited sustained exocytosis in the presence of intracellular ATP, suggesting that local metabolic control by mitochondria is critical for this phase. Taken together, my data indicate that Na^+/Ca^{2+} exchanger-mediated Ca^{2+} clearance mediated by NCLX and NCX is crucial for optimizing mitochondrial function, which in turn contributes to vesicle recruitment for sustained exocytosis in pancreatic β-cells.

Keywords: Pancreatic β-cell, Ca^{2+} transport, Na^+/Ca^{2+} exchanger, Exocytosis, Capacitance

Student Number: 2009-30617

CONTENTS

ABSTRACT.....i

CONTENTS..... iii

LIST OF FIGURES.....v

LIST OF ABBREVIATIONS..... vii

INTRODUCTION.....1

1. General description of insulin secretion mechanism in pancreatic β-cells 1

2. Regulation of intracellular Ca^{2+} in pancreatic β-cells.....2

3. Na^{+}/Ca^{2+} exchangers at the plasmalemma and mitochondria and their roles in regulating insulin secretion 3

4. Aim of the present study.....5

MATERIALS AND METHODS.....10

1. Cell Culture 10

2. Preparation of Mouse Pancreatic Tissue Section.....10

3. Ca^{2+} Measurements.....11

4. Immunofluorescence Staining 12

5. Western Blot Analysis and Biotinylation Experiment 14

6. NCLX Knockdown.....15

7. Capacitance Measurement.....15

8. Measurement of Mitochondrial Membrane Potential ($\Delta\Psi_m$).....16

9. Statistical Analysis.....17

RESULTS.....18

1. Role of plasma membrane NCLX in cytosolic Ca^{2+} dynamics.....18

2. Immunodetection of NCLX on the plasma membrane in pancreatic β-cells.....20

3. Role of NCLX on the Exocytosis Function.....22

4. Downregulation of NCLX induces mitochondrial dysfunction to suppress sustained exocytosis.....26

DISCUSSION.....48

REFERENCES.....56

ABSTRACT in KOREAN.....65

LIST OF FIGURES

Figure 1. Schematic diagram of glucose-stimulated insulin secretion (GSIS) in pancreatic β-cell. 7

Figure 2. The regulation of intracellular Ca^{2+} concentration..... 8

Figure 3. Ca^{2+} clearance after depolarization-induced Ca^{2+} increases is slowed by the replacement of Na^{+} with NMG^{+} more strongly than with Li^{+} in INS-1 cells. 30

Figure 4. Replacement of Na^{+} with NMG^{+} is more efficient than Li^{+} to facilitate Ca^{2+} influx mode of Na^{+}/Ca^{2+} exchange..... 31

Figure 5. The expression of NCLX on the plasma membrane in pancreatic β-cells. 33

Figure 6. Effect of NCLX knockdown on Ca^{2+} clearance and depolarization-induced exocytosis. 35

Figure 7. NCLX knockdown delays RRP recovery..... 37

Figure 8. Effect of intracellular Na^{+} on depolarization-induced exocytosis. . 39

Figure 9. Effect of inhibiting NCX and Na^{+} replacement on depolarization-induced exocytosis. 40

Figure 10. siNCLX or NCX inhibition by XIP does not affect voltage-

dependent Ca^{2+} currents. 41

Figure 11. The effect of NCLX knockdown on Ca^{2+} responses to ten depolarizations. 43

Figure 12. Effect of siNCLX or NCX inhibition by XIP on mitochondrial membrane potential. 44

Figure 13. Effect of oligomycin on depolarization-induced exocytosis..... 46

Figure 14. Schematic diagram for the role of NCLX in the exocytosis of pancreatic β-cell. 47

LIST OF ABBREVIATIONS

CaTs	Ca^{2+} transients
$[Ca^{2+}]_i$	intracellular (Cytosolic) Ca^{2+} concentration
Ctrl	control
ΔC_m	depolarization-induced cell capacitance increase
$\Delta \Psi_m$	mitochondrial membrane potential
ER	endoplasmic reticulum
GSIS	glucose-stimulated insulin secretion
GLUT 2	glucose transporter, type 2
Ins(1,4,5)P_3R	inositol-1,4,5-trisphosphate receptor
K_{ATP}	ATP-sensitive K^+
LTCC	L-type Ca^{2+} channel
mNCX	mitochondrial Na^+/Ca^{2+} exchanger
NCKX	K^+-dependent Na^+/Ca^{2+} exchanger
NCLX	Li^+-permeable Na^+/Ca^{2+} exchanger
NCX	Na^+/Ca^{2+} exchangers
NMG	N-methyl-D-glucamine
PMCA	Plasma membrane Ca^{2+}-ATPase

Q	value of Ca^{2+} influx
RRP	readily releasable pool
RyR	ryanodine receptor
SERCA	Sarco(endo)plasmic reticulum Ca^{2+}-ATPase
si	Small interfering
τ_{fast}^{-1}	fast rate constant
τ_{slow}^{-1}	slow rate constant
TMRM	Tetramethylrhodamine, methyl ester

INTRODUCTION

1. General description of insulin secretion mechanism in pancreatic β-cells

Pancreatic β-cells are the most abundant cell type (65~90%) of the islets of Langerhans which constitute 1%, or less, of the mass of the pancreas, and play important roles in maintaining glucose homeostasis by secreting insulin in response to elevated blood glucose levels (Ashcroft and Rorsman, 1989; Leibiger et al., 2008; MacDonald and Rorsman, 2006). The scheme for glucose-stimulated insulin secretion (GSIS) of pancreatic β-cell is shown in Fig. 1. When extracelluar glucose rises, the entry of glucose via glucose transporter, type 2 (GLUT 2) accelerates glucose metabolism by oxidative glycolysis, resulting in an increase in ATP content and ATP/ADP ratio. This altered ATP/ADP ratio causes the ATP-sensitive K^+ (K_{ATP}) channels to close, which elicits depolarization of the cell membrane and electrical activity, leading to the opening of L-type Ca^{2+} channels (LTCC) and Ca^{2+} entry. The raised intracellular calcium concentration ($[Ca^{2+}]_i$) triggers exocytosis on insulin-containing vesicles (Rorsman and Renstrom, 2003).

2. Regulation of intracellular Ca^{2+} in pancreatic β-cells

As described above, intracellular Ca^{2+} signaling plays a central role in pancreatic β-cell function (Ashcroft et al., 1994). Cytosolic Ca^{2+} concentration ($[Ca^{2+}]_i$) is tightly regulated by Ca^{2+} homeostatic mechanism (fig. 2). Ca^{2+} signals are modified by the control of Ca^{2+} flux in (entry) and out (efflux) of the cell through channels and transporters at plasma membrane. These proteins facilitate Ca^{2+} movement between the extracellular milieu and cytoplasm across a Ca^{2+} concentration gradient (Berridge et al., 2003). In addition, integral proteins localized in the membranes of intracellular stores, such as endoplasmic reticulum (ER) and mitochondria, allow Ca^{2+} release to the cytoplasm and reuptake into the Ca^{2+} stores (Berridge et al., 2000; Stutzmann and Mattson, 2011). Cell stimulation by agonist or membrane depolarization induces Ca^{2+} release from ER to cytosol through ryanodine (RyR) and inositol-1,4,5-trisphosphate receptor ($Ins(1,4,5)P_3R$), or Ca^{2+} entry to cytosol by opening of voltage-dependent Ca^{2+} channel (Berridge et al., 2003; Stutzmann and Mattson, 2011). Ca^{2+} removal from the cytosol is mediated by other Ca^{2+} transporters, including the NCX (Na^+/Ca^{2+} exchanger) and PMCA (Plasma membrane Ca^{2+}-ATPase) that extrude Ca^{2+} from the cytosol and SERCA (Sarco(endo)plasmic reticulum Ca^{2+}-ATPase) that transfers Ca^{2+} from the cytosol to the ER (Berridge

et al., 2003). Mitochondria sequester Ca^{2+} through an mitochondrial uniporter and mitochondrial Ca^{2+} might be then released slowly into the cytoplasm through the mitochondrial NCX (mNCX) (Berridge et al., 2000).

Considering that cytosolic Ca^{2+} concentration is regulated by various Ca^{2+} transporters such as NCX and mNCX, as well as Ca^{2+} pumps such as PMCA and SERCA, these Ca^{2+} transporters may have impacts on the exocytosis of β-cells (Chen et al., 2003; Gall et al., 1999; Herchuelz et al., 2002; Herchuelz et al., 2007; Hernández-SanMiguel et al., 2006; Hughes et al., 2006; Kamagate et al., 2002; Lee et al., 2003).

3. Na^+/Ca^{2+} exchangers at the plasmalemma and mitochondria and their roles in regulating insulin secretion

Mammalian Na^+/Ca^{2+} exchangers include three branches of much larger family of transport proteins: NCX, NCKX (K^+-dependent Na^+/Ca^{2+} exchanger), and NCLX (Li^+-permeable Na^+/Ca^{2+} exchanger) (Lytton, 2007). The Na^+/Ca^{2+} exchanger at the plasma membrane in pancreatic β-cells is encoded by NCX1 (NCX1.3 and NCX1.7), one of the three isoforms (NCX1, NCX2, and NCX3) of NCX (Hamming et al., 2008; Van Eylen et al., 1997). NCX is one of the major Ca^{2+} clearance mechanisms in pancreatic β-cells (Chen et al., 2003;

Herchuelz et al., 2002), and they are emerged as important targets for the regulation of insulin secretion. It was reported that inhibition of NCX with KB-R7943 or shRNA-mediated downregulation of NCX1 enhanced glucose-induced Ca^{2+} responses, depolarization-induced exocytosis, and GSIS in mouse pancreatic β-cells (Hamming et al., 2010). However, NCX may also operate in Ca^{2+} influx mode (reverse mode), especially at depolarized membrane potentials, and there is a report to support such action; Knockdown of NCX1 with antisense oligonucleotides in rat pancreatic β-cells significantly inhibited Ca^{2+} increases by high K^+, sulfonylurea, or high glucose, suggesting that NCX contributes to Ca^{2+} entry during membrane depolarization, thus contributing to insulin secretion (Van Eylen et al., 1998).

Mitochondria play important roles in metabolism-secretion coupling in β-cells (Wiederkehr and Wollheim, 2008). mNCX acts as a Ca^{2+}-releasing pathway from the mitochondria into the cytosol in exchange for Na^+ influx (Bernardi, 1999; Crompton and Heid, 1978). mNCX are also considered as important regulator of insulin secretion (Lee et al, 2003). The inhibitor of mNCX, the benzothiazepine compound CGP-37157, in INS-1 cells increased glucose-induced increase in mitochondrial Ca^{2+}, cellular ATP contents, and glucose-induced insulin secretion (Lee et al., 2003). The increase of

mitochondrial matrix Ca^{2+} during the inhibition of mNCX may enhance mitochondrial energy metabolism via the activation of Ca^{2+}-dependent dehydrogenases in the TCA cycle. A molecular determinant of mNCX was recently identified as NCLX (Palty et al., 2010). NCLX is highly expressed in the rat pancreas (Palty et al., 2004). Downregulation of NCLX by small interfering RNA (siRNA)-mediated knockdown resulted in a delay of GSIS, suggesting that NCLX activity is required for normal GSIS (Nita et al., 2012). In spite that NCLX is considered to encode mNCX, the discrepancy between the effects of pharmacological block of mNCX and knockdown of NCLX on insulin secretion may imply that NCLX may have other functions than mNCX. NCLX was originally reported as a Na^{+}/Ca^{2+} exchanger at the plasma membrane (Cai and Lytton, 2004; Palty et al., 2004), suggesting a possibility that NCLX is not exclusively targeted to the mitochondrial membrane.

4. Aim of the present study

To understand the function of NCLX in pancreatic β-cells, I specifically investigated following questions: 1) Is there evidence for the presence of NCLX at the plasma membrane?, 2) Does NCLX contribute to the regulation of cytosolic Ca^{2+}, and if so, what is its contribution compared to NCX?, 3) Do

NCLX and NCX contribute to insulin secretion, and if so, what is the underlying mechanism?, 4) Can we distinguish the role of plasmalemmal NCLX and mitochondrial NCLX in regulating insulin secretion?

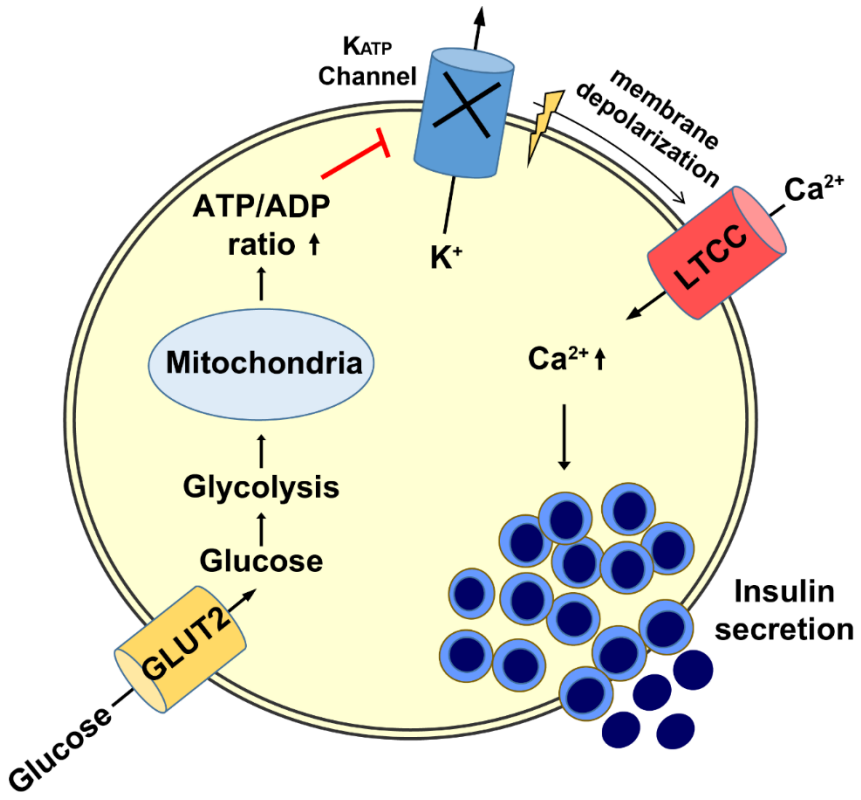

Figure 1. Schematic diagram of glucose-stimulated insulin secretion (GSIS) in pancreatic β-cell.

In the pancreatic β-cell, the glucose transporter (GLUT 2) facilitates the uptake of glucose into the cell and the glycolytic phosphorylation of glucose causes a rise in the ATP:ADP ratio. This rise leads to the closure of ATP-sensitive K^+ (K_{ATP}) channel and membrane depolarization, resulting in the opening of L-type Ca^{2+} channel (LTCC) and the raised intracellular Ca^{2+} concentration ($[Ca^{2+}]_i$). The rise in levels of calcium ions leads to the exocytotic release of insulin from storage granule.

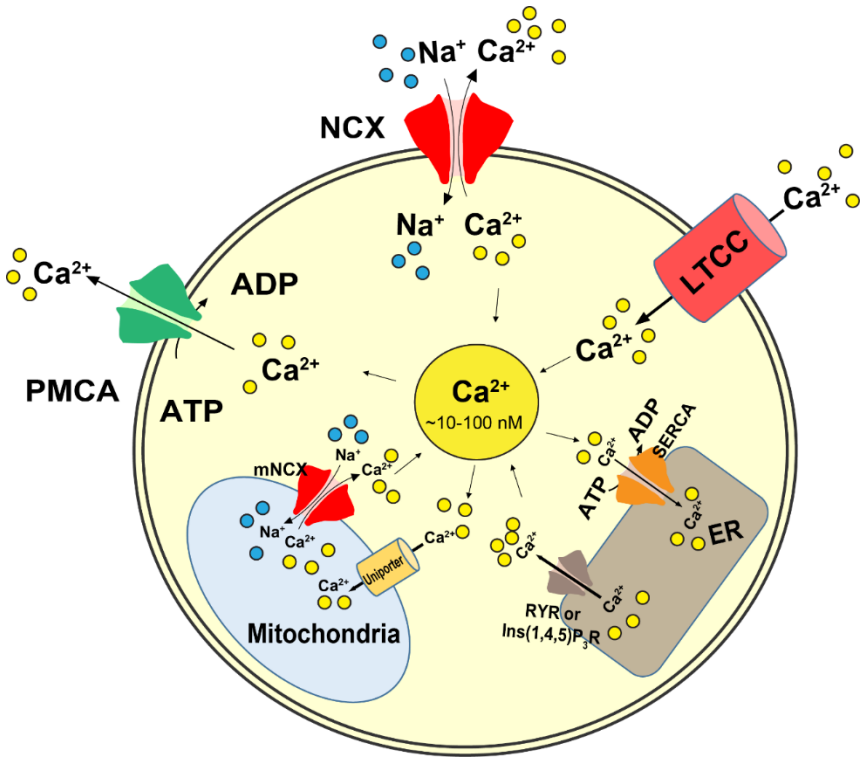

Figure 2. The regulation of intracellular Ca^{2+} concentration.

Schematic diagram that highlights Ca^{2+} channel and Ca^{2+} transporters implicated in Ca^{2+} homeostasis. Ca^{2+} enters into the cell through voltage-gated Ca^{2+} channel. Ca^{2+} is extruded from the cytosol through NCX (Na^+/Ca^{2+} exchanger), PMCA (Plasma membrane Ca^{2+}-ATPase), SERCA (Sarco(endo)plasmic reticulum Ca^{2+}-ATPase) and mitochondrial uniporter. Release of Ca^{2+} from endoplasmic reticulum (ER) store or mitochondria to cytosol is mediated through the ryanodine (RyR) and inositol-1,4,5-trisphosphate receptors ($Ins(1,4,5)P_3R$) or mitochondrial Na^+/Ca^{2+} exchangers

(mNCX). Intracellular Ca^{2+} concentration is tightly regulated by Ca^{2+} homeostasis mechanism.

MATERIALS AND METHODS

1. Cell Culture

Rat insulinoma INS-1 cells (passage 20-50) were cultured as previously described (Lim et al., 2009). Cells were cultured in RPMI medium containing 10% fetal bovine serum, 11.1 mM $_{D}$-glucose, 2 mM L-glutamine, 100 units/ml penicillin, and 100μg/mL streptomycin, 50 μM β-mercaptoethanol in a humidified incubator supplied with 5% CO_2 at 37 ºC. Cells were plated on poly-$_{L}$-lysine-coated coverslips at $5x10^4$ for immunocytochemical studies and on 12-well plates at a density of $5x10^4$ per well for electrophysiological experiments.

2. Preparation of Mouse Pancreatic Tissue Section

Female C57BL/6 mice at 7-8 weeks were sacrificed and pancreata were removed quickly and fixed in 10% formalin and paraffin embedded for serial sectioning (5 μm thick). All experimental procedures were conducted in accordance with the guidelines of the University Committee on Animal Resources at Seoul National University (Approval No: SNU-130611-4).

3. Ca^{2+} Measurements

Cytosolic Ca^{2+} concentrations ($[Ca^{2+}]_i$) were measured with Fura-2. 4 μM Fura-2 AM (Invitrogen, Eugene, OR, USA) were loaded for 30 min to measure the Ca^{2+} signal from the intact cells. The extracellular solutions contained in mM: 143 NaCl, 5.4 KCl, 5 HEPES, 0.5 $MgCl_2$, 1.8 $CaCl_2$, 5 glucose, pH 7.4. 200 μM diazoxide (Sigma, St. Louis, Mo., USA), a K_{ATP} channel activator, was added to the extracellular solution for the Ca^{2+} measurement in intact cells. For whole-cell voltage clamp experiments, 50 μM Fura-2 was added to the internal solution which contained in mM: 110 K-aspartate, 30 KCl, 10 HEPES, 1 $MgCl_2$, 5 MgATP, 0.1 NaGTP, pH 7.2. The extracellular NaCl was reduced to 20 mM during inhibition of plasma membrane Na^+/Ca^{2+} exchanger activity (pNCEx) by replacing it with NMG-Cl or LiCl. Cells were placed to a chamber mounted on an inverted microscope (IX71S1F-2, Olympus, Tokyo, Japan) and observed with a 40x water immersion objective (UApo/340, NA 1.15; Olympus). Fura-2 was excited with alternative 340 and 380 nm monochromatic lights generated by Polychrome V (Till Photonics, Grafelfing, Germany) and the emitted lights >470 nm were collected with a digital camera (sCMOS Neo, Andor Technology, Belfast, UK) or a photometry system (Till Photonics) using Metafluor (Molecular Devices, Downingtown, PA, USA) or PULSE softwares (HEKA

Elektronik, Lambrecht, Germany). Fura-2 fluorescence was calibrated using in-cell calibration method by measuring maximum and minimum ratio at high and low Ca^{2+} containing solutions. The Ca^{2+} concentration was then calculated according to the following equation.

$$[Ca^{2+}]_i = K_d*(Sf2/Sb2)*(R-R_{min})/(R_{max}-R)$$

,where K_d, 224 nM; Sf2 and Sb2, maximum and minimum fluorescence values at 380 nm; R, ratio of F380/F340; R_{min} and R_{max}, minimum and maximum Fura-2 ratio values, respectively. The R_{min} and R_{max} were obtained using 10 mM EGTA or 15 mM Ca^{2+} containing solutions.

4. Immunofluorescence Staining

For INS-1 cell surface NCLX staining, cells were incubated with goat polyclonal anti-NCLX antibody (1:50; Santa Cruz Biotechnology, Santa Cruz, CA, USA) in serum-free and antibiotic-free RPMI culture medium for 1 h at 4°C and quickly washed with culture medium, fixed with ice-cold 4% paraformaldehyde in PBS for 15 min, and washed with PBS. Cells were blocked with 5% donkey serum in PBS for 1h at room temperature. Then cells were incubated for 1 h in blocking solution of Cy5-conjugated donkey anti-goat IgG (1:100; Jackson Immunoresearch Laboratories, West Grove, PA, USA).

After washing, the cells were mounted with Gel Mount (Biomeda Corp, Foster City, Calif., USA) on slides. For negative controls, cells were stained secondary antibody alone (Cy5-conjugated donkey anti-goat IgG alone) or 20μg of primary antibody (goat polyclonal anti-NCLX antibody) preabsorbed with 40 μg of blocking peptide for 2h at room temperature. For mouse pancreatic tissue sections staining, paraffin-embedded sections were incubated for 40 min at 55°C and deparaffinized in xylen and rehydrated through serial ethanol to distilled water. After the sections were placed in the heat-induced antigen solution for 20 min, the sections were blocked with 5% bovine serum albumin, 0.3% Triton X-100 in PBS for 1h at room temperature. Tissue sections were sequentially double-stained by combining goat polyclonal anti-NCLX antibody (1:50; Santa Cruz Biotechnology), and mouse monoclonal anti-glucagon antibody (1:500; Sigma) in blocking solution overnight at 4°C, and then washed. The sections were thereafter incubated with Alexa 633 donkey anti-goat IgG (1:200; invitrogen) and FITC-conjugated donkey anti-mouse IgG (1:200; Jackson ImmunoResearch) in blocking solution for 1h at room temperature and rinsed with PBS and mounted with fluorescence mounting medium (Dako, Glostrup, Denmark). Images were acquired by TCS-SP2 confocal laser-scanning microscope (Leica, Heidelberg, Germany) with 40x or 63x water

immersion objective, and processed using Leica Confocal Software (Leica). The same instrument settings were used for each experiment.

5. Western Blot Analysis and Biotinylation Experiment

The total and cell surface expression of NCLX were determined using NCLX antibody (1:100, Santa Cruz Biotechnology), which is a goat polyclonal antibody raised against a peptide mapping within an N-terminal extracellular domain of NCKX6 (NCLX). To detect cell surface NCLX, the cell surface proteins were pulled down after biotinylation using EZ-Link Sulfo-NHS-SS-Biotin kit (Pierce, Rockford, IL, USA) according to manufacturer's guideline as described previously (Lim et al., 2009). The protein samples were resolved using 10% SDS-PAGE and transferred onto a polyvinylidene difluoride membrane (Millipore). The blotted membrane was blocked with 5% skim milk, 0.2% Tween-20 in PBS overnight at 4°C and incubated with NCLX antibody for 2h at room temperature. After washing, the membrane was incubated with secondary donkey anti-goat IgG-HRP (1:2500, Santa Cruz Biotechnology) for 1h at room temperature. Detection was performed with Amersham ECL Plus Western Blotting Detection Reagents (GE Healthcare, Piscataway, NJ, USA) and blots were exposed to the X-ray film. For negative control, I used

preabsorbed primary antibody as describe above.

6. NCLX Knockdown

To suppress NCLX expression, I purchased the silencer select siRNAs targeted aginst NCLX (5'-GAUCAGAUGUCUUCCAACAtt-3') from ambion (Austin, TX, USA). siGFP (5'-GCAAGCUGACCCUGAAGUUCAU-3') was used as the control siRNA as previously described (Park et al., 2013). 70% confluent INS-1 Cells in 12-well plate were co-transfected with siGFP or siNCLX and DsRed reporter vector using Lipofectamine 2000 reagent (Invitrogen) according to the instructions of the manufacturer and experiments were performed 48 h after transfection.

7. Capacitance Measurement

Cell capacitance, C_m, was monitored in a whole cell configuration with "sine+dc" mode using a built-in lock-in extension module of EPC10 amplifier and Patchmaster software (HEKA Elektronik). A 10-consecutive depolarizations from a holding potential -70 to 0 mV were given to induce Ca^{2+} influx and exocytosis. In-between the depolarizations, cells were stimulated with sinewaves with 10 mV peak amplitude and 1 kHz frequency to calculate

C_m. Extracellular solution contained in mM: 123 NaCl, 20 TEA-Cl, 5.4 KCl, 5 HEPES, 0.5 $MgCl_2$, 1.8 $CaCl_2$, 5 glucose, pH 7.4. The extracellular NaCl was reduced to 20 mM during inhibition of plasma membrane Na^+/Ca^{2+} exchanger activity (pNCEx) by replacing it with NMG-Cl or LiCl. Internal pipette solution contained in mM: 125 Cs-glutamate, 20 CsCl, 5 HEPES, 1 $MgCl_2$, 3 MgATP, 0.05 EGTA or 0.05 Fura-2 free acid, pH 7.2. 10 mM CsCl was replaced with equimolar NaCl in some experiments. Experiments were performed at 35 ºC. ΔC_m was normalized by initial cell capacitance (fF/pF). The range of cell capacitance is from 6 to 14 pF (9.53 ± 0.29 pF, n = 62).

8. Measurement of Mitochondrial Membrane Potential ($\Delta\Psi_m$)

The changes in mitochondrial membrane potential ($\Delta\Psi_m$) was monitored by cell-permeant, membrane potential sensitive dye, Tetramethylrhodamine, methyl ester (TMRM: excitation wavelength maximum at 549 nm, emission wavelength at 573 nm, invitrogen). Cells were loaded with 2 μM TMRM for 30 min at 37 ºC and 10nM TMRM was added to the extracellular solution during recording. I monitored TMRM fluorescence in dequenching mode and increase in TMRM fluorescence reflects depolarization of $\Delta\Psi_m$ (Voronina et

al., 2004). Cells were transferred to a chamber mounted on the same microscope as describe above. TMRM was excited at 530 nm with a high-powered LED source and a driver (LED4C2 and DC4100; Thorlabs, Newton, NJ, USA) and the emitted lights >590 nm were collected using a cooled digital camera (sCMOS Neo; Andor Technology) and acquisition software (MetaFluor; Molecular Devices). An image was collected every 500 ms. TMRM fluorescence is presented as F/F_0, where F is the fluorescence intensity at each time point and F_0 is averaged resting fluorescence before the depolarizing pulse and averaged TMRM fluorescence changes is defined as percent increase from initial levels before the depolarizing pulse.

9. Statistical Analysis

Data were expressed as means ± S.E.M. The statistical differences between the experimental groups were analyzed using paired or unpaired two-sampled Student's t-test or ANOVA. A P value of < 0.05 was considered as statistically significant.

RESULTS

1. Role of plasma membrane NCLX in cytosolic Ca^{2+} dynamics

To characterize the contribution of Na^+/Ca^{2+} exchangers to the Ca^{2+} clearance in INS-1 cells, I compared the effect of Na^+ replacement with N-methyl-D-glucamine (NMG) and that with Li^+ on cytosolic Ca^{2+} transients (CaTs) using Fura-2 fluorescence Ca^{2+} indicator. I elicited CaTs by applying a 500 ms depolarization pulse to 0 from -70 mV, and measured the effect of Na^+ replacement on the decay phase of CaTs upon repolarization to -70 mV (Fig. 3). To rule out the influence of mNCX activity on CaTs, I used a Na^+-free internal solution. To observe the difference in Ca^{2+} clearance in different solutions, each Ca^{2+} transient obtained in the solutions was normalized to its peak, and the decay phase was compared (Fig. 3A). The decay phase was slowed by replacing 123 mM external Na^+ with Li^+ or NMG^+, and the slowing was more profound using NMG^+ than Li^+. The fact that the Li^+ was less effective than NMG^+ for inhibiting Ca^{2+} clearance suggested the presence of NCLX at the plasma membrane of INS-1 cells. For quantitative analysis, I fitted the decay phase of CaT with a double exponential function and fast and slow

rate constants (τ_{fast}^{-1} and τ_{slow}^{-1}) for Ca^{2+} decay were obtained. Na^+ replacement with Li^+ or NMG^+ reduced τ_{fast}^{-1} significantly, but did not affect τ_{slow}^{-1}, suggesting that Na^+/Ca^{2+} exchanger activity contributes to the fast phase of Ca^{2+} decay (Fig. 3B). The reduction of τ_{fast}^{-1} in Li^+ represented the contribution of NCX to the Ca^{2+} clearance, which was 39%. The reduction of τ_{fast}^{-1} in NMG^+ represented the contribution of total Na^+/Ca^{2+} exchanger activity (64.2%), which was attributable to NCX and NCLX; the contribution of NCLX was calculated to be 25.2%.

I then examined the contribution of NCX and NCLX to the reverse mode of Na^+/Ca^{2+} exchange activity, which was monitored by the Ca^{2+} increases induced by the total replacement of extracellular Na^+ with Li^+ or NMG^+. To inhibit the possible Ca^{2+} influx through L-type Ca^{2+} channels, I added L-type Ca^{2+} channel inhibitor, nimodipine (10 μM), throughout the experiments. Repetitive application of Na^+-free solutions induced increases in cytosolic Ca^{2+} to the similar level (Fig. 4A and B). The amplitude of Ca^{2+} increase ($\Delta[Ca^{2+}]_i$) in NMG^+ was significantly larger than that in Li^+ (62.45 ± 8.89 nM vs. 35.71 ± 6.66 nM; $P < 0.001$) (Fig. 4C and D), suggesting that the Ca^{2+} influx mediated by NCLX is about 42.8% of the total Ca^{2+} influx mediated by the reverse mode of total Na^+/Ca^{2+} exchanger activity.

It is controversial whether NCLX activity is dependent on the presence of K^+ (Cai and Lytton, 2004; Palty et al., 2004). Since K^+ concentrations also affect Na^+/K^+ pump, I tested the effects of external K^+ (5 mM) on the Ca^{2+} increases induced by extracellular Na^+ replacement with NMG^+ while plasma membrane Na^+/K^+ pump was inhibited with 1 mM ouabain. Under this condition, the amplitude of $\Delta[Ca^{2+}]_i$ induced by extracellular Na^+ replacement with NMG^+ became larger, suggesting that cytosolic Na^+ accumulation by inhibiting Na^+/K^+ pump increases Ca^{2+} influx mediated by the reverse mode of Na^+/Ca^{2+} exchange (Fig. 4E). However, the amplitude of $\Delta[Ca^{2+}]_i$ was not affected by the removal of extracellular K^+ (Fig. 4E and F), suggesting that neither NCX nor NCLX is K^+-dependent.

2. Immunodetection of NCLX on the plasma membrane in pancreatic β-cells

Previous report showed that the NCLX is highly expressed in pancreatic tissues (Palty et al, 2004), but its localization in the pancreas was not shown. To confirm whether NCLX is expressed in pancreatic β-cells, I further examined the distribution of NCLX expression in the paraffin-imbedded slice preparation of mouse pancreatic tissue. The results show that the expression

level is higher in islet cells than the nearby exocrine cells (Fig. 5A). NCLX expression in glucagon-positive α cells appeared to be negligible, suggesting that a high expression of NCLX is selective to pancreatic β-cells.

Previously, the NCLX have been originally found to mediate Ca^{2+} transport in the plasma membrane (Cai & Lytton, 2004; Palty et al, 2004). However, after finding that mNCX is mediated by NCLX (Palty et al, 2010), researches are focused on the mitochondrial NCLX function. Since my functional Ca^{2+} dynamics data suggest the presence of NCLX on the plasma membrane, I further examined whether the NCLX protein is indeed detected in the plasma membrane by using NCLX specific antibody in immunocytochemistry and biotinylation experiments. The intact INS-1 cells were incubated with antibody against N-terminal extracellular domain of NCLX, for 1 h at 4 ºC without permeabilization or fixation. The antibody was incubated at low temperature to decrease possible nonspecific reaction and inhibit endocytosis of bound antibodies. Confocal images show that the NCLX antibody and Cy5-conjugated secondary antibody were detected at cell surface under nonpermeabilized condition (Fig. 5B). When INS-1 cells were permeabilized, NCLX proteins were observed scattered in the cytoplasm, suggesting the presence of NCLX in the intracellular compartments, such as mitochondria (Fig. 5B). To further

confirm the existence of NCLX in the plasma membrane, the cell surface proteins were pulled down after biotinylation and performed western blot analysis for NCLX. Figure 5C shows immunoblot of NCLX from cell surface proteins. The size of cell surface NCLX is about 64 kDa, suggesting that the NCLX expressed in the cell surface is a full length form. These immuno-detections of cell surface NCLX are not due to a nonspecific binding of primary or secondary antibodies to the other plasma membrane proteins because incubation of the primary antibodies in the presence of the NCLX blocking peptides or secondary antibodies alone showed no detectable signals (Fig. 5B and C). Taken together, out data show that NCLX is highly expressed in the pancreatic β-cells and present not only in the intracellular compartments but also at the plasma membrane.

3. Role of NCLX on the Exocytosis Function

I investigated the role of NCLX in exocytosis using siNCLX-transfected INS-1 cells. Endogenous NCLX expression was decreased in siNCLX-transfected cells than in control siRNA (siCtrl)-transfected cells (Fig. 6A). To ensure the functionality of NCLX as a plasmalemmal Na^+/Ca^{2+} exchanger, I examined Ca^{2+} decay rate, and confirmed that τ_{fast}^{-1} was reduced by 26.9% in

siNCLX-transfected cells compared to siCtrl-transfected cells (Fig. 6B and C). There was no significant difference in resting Ca^{2+} level between siCtrl- and siNCLX-transfected cells (siCtrl, 0.10 ± 0.02 μM vs siNCLX, 0.14 ± 0.04 μM). Membrane capacitance of INS-1 cells transfected with siCtrl and with siNCLX were 9.73 ± 0.75 pF (*n*=12) and 8.86 ± 0.77 pF (*n*=12), respectively, and these values were not significantly different. Exocytosis was induced by a train of ten successive depolarization pulses with 500 ms duration in a 500 ms interval and changes in membrane capacitance (ΔC_m) were measured (Fig. 6D). As was demonstrated in previous studies using mouse pancreatic β-cells (Kang et al., 2006; Kanno et al., 2004), exocytosis proceeded throughout the train in INS-1 cells (Fig. 6D). Interestingly, when the cumulative plot for the C_m increment was compared between siCtrl and siNCLX-transfected cells, I found that the C_m increment during first two pulses was not different, whereas the responses to the later pulses were significantly reduced in siNCLX-transfected cells (Fig. 6E). Since a significant difference was observed from the C_m increment by the 3rd pulse, I obtained the sum of the C_m increments induced by the 3rd to 10th pulses ($\Delta C_{m3\text{-}10}$) for quantitative analysis, and confirmed that $\Delta C_{m3\text{-}10}$ was significantly smaller in siNCLX-transfected cells (siCtrl, 37.9 ± 5.72 fF/pF *vs* siNCLX, 12.31 ± 1.46 fF/pF; $P < 0.001$) (Fig. 6F).

It is generally believed that the initial response during a train of depolarization reflects the exocytosis from a subset of the readily releasable pool (RRP) situated close to the voltage-gated Ca^{2+} channels, whereas the late response reflects sustained release supported by the recruitment of vesicles to the vicinity of Ca^{2+} channels or the vesicle priming reaction (Barg et al., 2002; Barg et al., 2001a; Barg et al., 2001b; Kang et al., 2006). To examine whether selective inhibition of the late response by siNCLX is attributable to the inhibition of vesicle recruitment or priming, I examined whether the recovery of RRP is affected by siNCLX. After depleting RRP using two successive depolarization pulses (500 ms duration, 500 ms interval), the same double pulses were applied with variable intervals (10–300 s) (Fig. 7A). The sum of C_m increment by the second double pulses ($\Delta C_{m1\text{-}2}$) increased as the interval increased, with the time constant (τ) of 73.3 s under control conditions, but the recovery time course was delayed significantly in siNCLX-transfected cells (τ, 150.6 s) (Fig. 7A and B), indicating that NCLX activity is required for vesicle recruitment or priming.

I performed the above experiments in a Na^+-free internal solution to minimize the mNCX activity. However, it is still not clear whether the effects of siNCLX on exocytosis is attributable to the inhibition of Na^+/Ca^{2+} exchange

activity across the plasma membrane or the mitochondrial membrane. To make this point clear, I investigated the role of mitochondrial NCLX in regulating depolarization-induced exocytosis by testing the effect of facilitating mitochondrial NCLX activity through the addition of Na^+ (10 mM) to the internal solution (Fig. 8). Intracellular concentrations of Na^+ had no significant effect on ΔC_m induced by a train of depolarization (Fig. 8A-C) and the time course of RRP recovery (Fig. 8D and E), suggesting that the role of mitochondrial NCLX in depolarization-induced exocytosis is negligible. These results support the idea that the effects of siNCLX is attributable to the inhibition of Na^+/Ca^{2+} exchange activity across the plasma membrane.

I showed that NCX as well as NCLX contributes to Ca^{2+} clearance in INS-1 cells (Fig. 3). Thus, I investigated the contribution of NCX to depolarization-induced exocytosis using XIP, an inhibitory peptide to NCX. Notably, XIP reduced sustained release ($\Delta C_{m3\text{-}10}$; 34.56 ± 4.59 fF/pF in control *vs* 13.9 ± 1.93 fF/pF in XIP, $P < 0.01$, but had no effect on the first two pulses (Fig. 9). The resemblance of the effects of XIP on depolarization-induced exocytosis to those of siNCLX strongly supports that Na^+/Ca^{2+} exchange activity across the plasma membrane is crucial for sustained insulin release.

The next question is whether the inhibitory effect of siNCLX or XIP on

depolarization-induced exocytosis is attributable to inhibition of forward-mode operation (Ca^{2+} clearance mode) or inhibition of reverse-mode operation (Ca^{2+} influx mode). To distinguish between these two possibilities, I tested the effect of Na^{+} reduction from external solutions on ΔC_m, which may inhibit the forward-mode but increase the reverse-mode of the exchanger activity. In NMG^{+} solutions, sustained release was similarly suppressed as shown in siNCLX or XIP-treated cells (Fig. 9). These results suggest that the inhibitory effect of inhibiting NCLX or NCX on vesicle exocytosis is likely attributable to the impairment of Ca^{2+} clearance.

4. Downregulation of NCLX induces mitochondrial dysfunction to suppress sustained exocytosis

The last question was how the impairment of Ca^{2+} clearance through the plasma membrane affects depolarization-induced exocytosis. One possibility is that impaired Ca^{2+} clearance accelerates Ca^{2+}-dependent inactivation of voltage-dependent Ca^{2+} currents. To exclude the possibility that the inhibitory effect of siNCLX or XIP on exocytosis is attributable to inhibition of voltage-dependent Ca^{2+} currents, I examined whether siNCLX or XIP affected Ca^{2+} influx changes (Fig. 10). The value of Ca^{2+} influx (Q) was calculated from the

integral of Ca^{2+} currents induced by depolarizing pulses. Q was unaffected either by siNCLX (Fig. 10A and B) or XIP (Fig. 10C and D), indicating that the inhibitory effects of siNCLX and XIP on depolarization-induced exocytosis are not attributable to the inhibition of Ca^{2+} currents. I also measured intracellular Ca^{2+} concentrations during ten depolarizing pulses and found a slight increase in siNCLX-transfected cells, especially in the later phase (Fig. 11A and B). The average Ca^{2+} concentrations during the later half in siNCLX-trnasfected cells was 13.5% larger than that in siCtrl-transfected cells, though statistical significance was not evident (P=0.053, Fig. 11C). These results indicate that the inhibitory effects of suppressing Na^{+}/Ca^{2+} exchange activity on the sustained phase of depolarization-induced exocytosis are not attributable to the inhibition of Ca^{2+} currents or decreased intracellular Ca^{2+} concentrations.

Since the sustained insulin release in response to a train of depolarization is known to be dependent on intracellular ATP (Eliasson et al, 1997; Rorsman et al, 2000), I hypothesized that the altered Ca^{2+} homeostasis caused by Na^{+}/Ca^{2+} exchanger activity inhibition may induce impaired cellular metabolism, and in turn, reduce ATP production. Therefore, I investigated whether inhibition of Na^{+}/Ca^{2+} exchanger activity might affect mitochondrial function. As an indicator of mitochondrial function, I measured changes in mitochondrial

membrane potential during a train of depolarization pulses. TMRE was loaded with a high concentration (2 μM) where the increase in TMRM fluorescence reflects mitochondrial depolarization (dequenching mode). In control INS-1 cells and in control siRNA-transfected cells, the TMRM fluorescence intensity increased rapidly upon depolarization but soon returned to the original level (Fig. 12), suggesting that mitochondrial membrane potential is slightly depolarized in response to the rise of cytosolic Ca^{2+} but the change is transient. In siNCLX-transfected cells, the increase of TMRM fluorescence intensity was much larger (17.03 ± 5.83 % increase in siCtrl, n=12; 35.35 ± 5.48 % increase in siNCLX, n=10; $P < 0.05$, Fig. 12A), and the recovery was much slower. Similarly, NCX-1 inhibition by XIP increased TMRM fluorescence intensity changes (16.64 ± 3.75 % increase in control, n=9; 43.42 ± 6.96 % increase in XIP, n=8; $P < 0.01$, Fig. 12B). These results suggest that impairment of Ca^{2+} clearance due to inhibition of NCLX or NCX induces mitochondrial dysfunction, which in turn inhibits the sustained phase of depolarization-induced exocytosis.

I also examined whether the inhibition of mitochondrial ATP synthesis indeed affects the sustained phase of depolarization-induced exocytosis under my experimental condition where 3 mM ATP is included in the internal solution.

Surprisingly, oligomycin, a mitochondrial ATP synthase inhibitor, selectively and significantly suppressed the sustained insulin release. These results suggest that local ATP production by mitochondria critically regulates the vesicle recruitment, and that impaired mitochondrial function results in impaired vesicle recruitment even though the global ATP level is maintained by the ATP-containing internal solutions (Fig. 13).

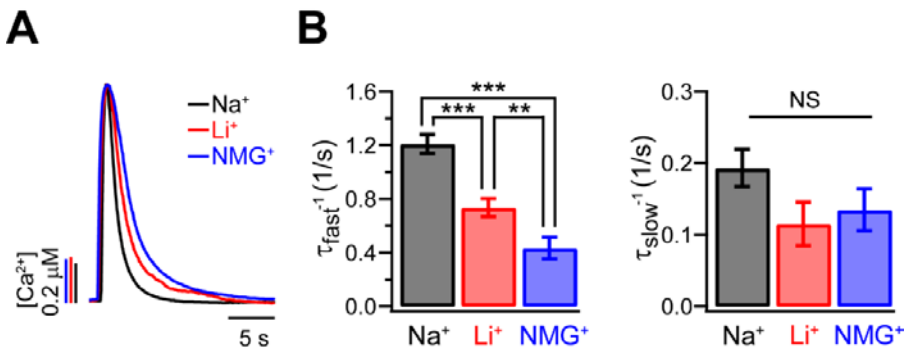

Figure 3. Ca^{2+} clearance after depolarization-induced Ca^{2+} increases is slowed by the replacement of Na^+ with NMG^+ more strongly than with Li^+ in INS-1 cells.

(A) A representative Ca^{2+} transient (CaT) induced by depolarizing pulse. External Na^+ (black) was replaced with Li^+ (red) and NMG^+ (blue). **(B)** Mean values for fast and slow decay rate constants (τ_{fast}^{-1} and τ_{slow}^{-1}) of CaT under the conditions indicated (Na^+ n=27; Li^+ n=13; NMG^+ n=9). $^{**}p<0.01$ and $^{***}p<0.001$ compared as indicated. NS, not significant.

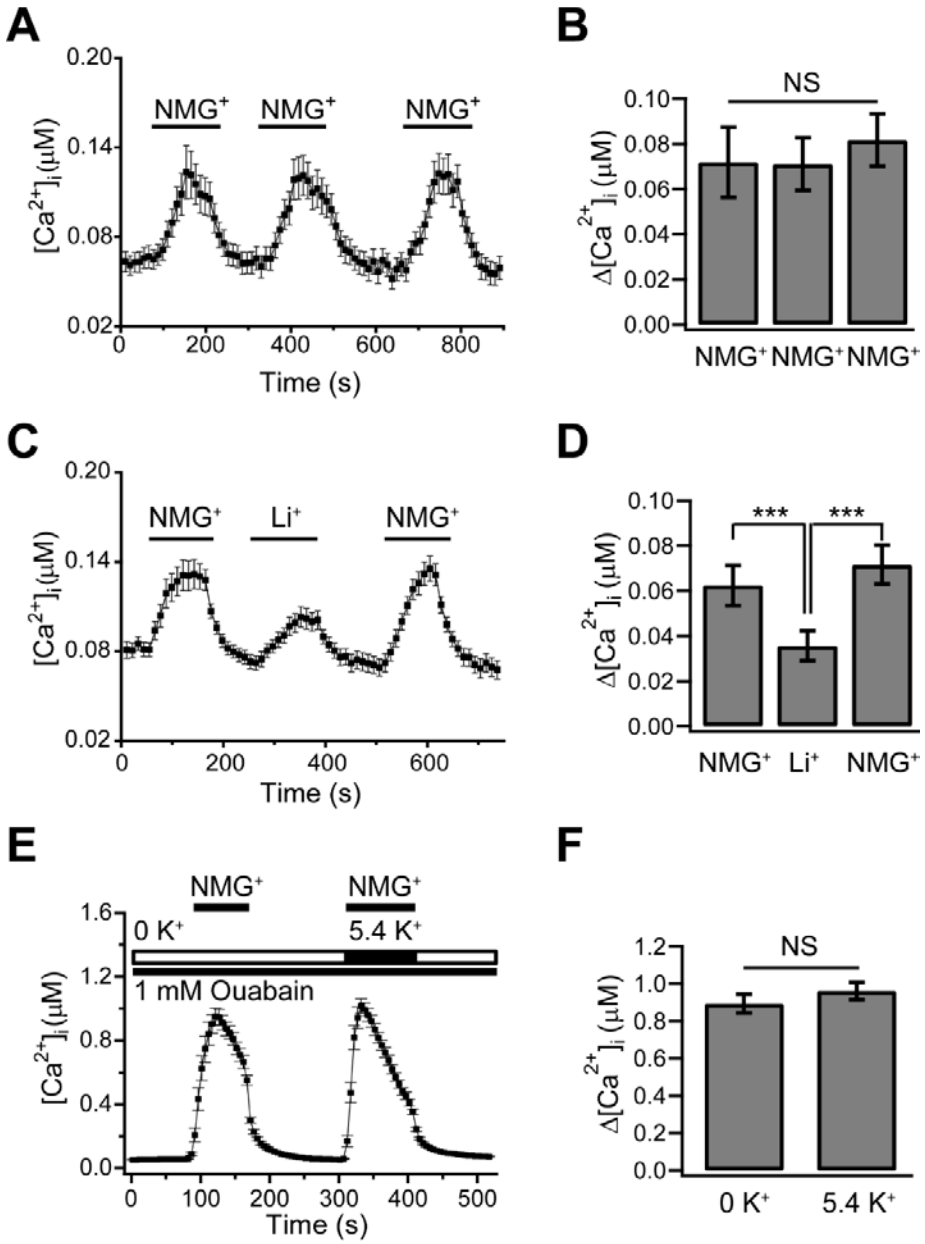

Figure 4. Replacement of Na^+ with NMG^+ is more efficient than Li^+ to facilitate Ca^{2+} influx mode of Na^+/Ca^{2+} exchange.

Figure 4. Replacement of Na^+ with NMG^+ is more efficient than Li^+ to facilitate Ca^{2+} influx mode of Na^+/Ca^{2+} exchange.

Averaged $[Ca^{2+}]_i$ signals in intact cells during replacement of extracellular Na^+ with **(A)** NMG^+ (*n*=12) or **(C)** NMG^+ followed by Li^+ (*n*=16) or **(E)** NMG^+ with or without extracellular K^+ (*n*=35) in the presence of nimodipine. The application of 1 mmol/l ouabain is indicated by a line. **(B, D, F)** Averaged peak $[Ca^{2+}]_i$ level ($\Delta[Ca^{2+}]_i$) from trace shown in **(A, C, E)**, respectively. $\Delta[Ca^{2+}]_i$ was calculated as the increment from the basal level. ***$p<0.001$ (paired *t*-test) compared as indicated. NS, not significant.

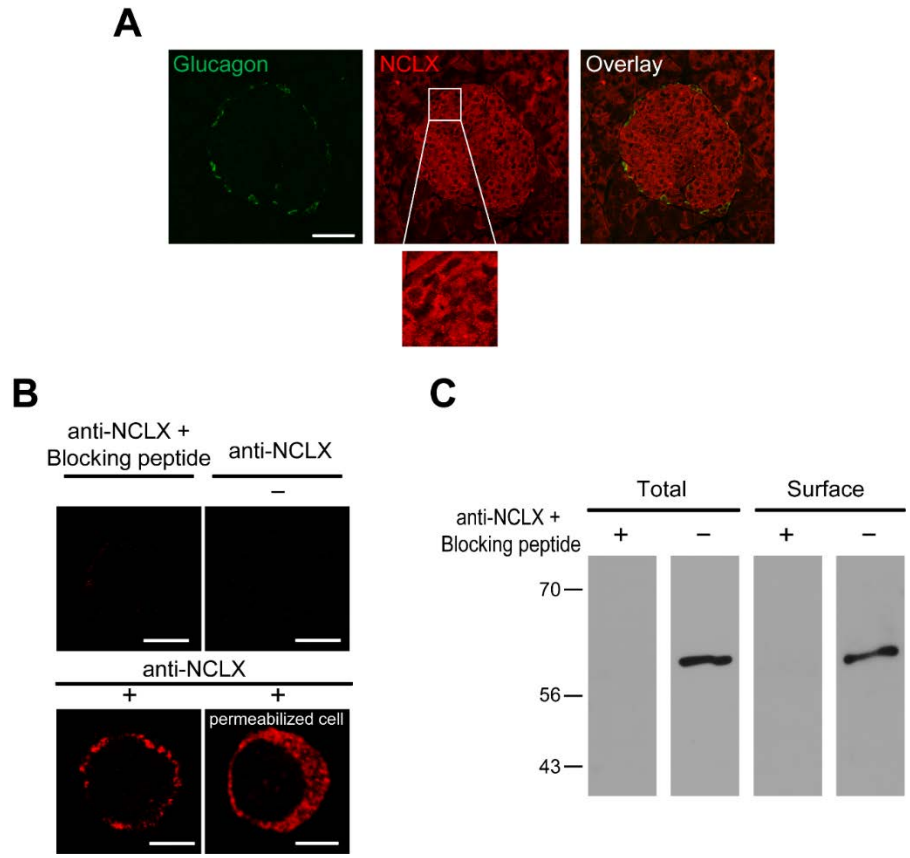

Figure 5. The expression of NCLX on the plasma membrane in pancreatic β-cells.

(A) Immunofluorescence analysis of mouse pancreas section using anti-NCLX antibody and anti-glucagon antibody. Scale bar, 50 μm. **(B)** Confocal images showing surface-immunostained with anti-NCLX antibody in INS-1 cells. Surface expression of NCLX was shown, but was undetected in the negative control immunolabeled using anti-NCLX antibody pre-incubated with NCLX blocking peptide or using Cy5-conjugated secondary antibody only. Scale bar,

5 μm. **(C)** Western blot analysis of total and biotin-labeled surface NCLX in INS-1 cells. Surface fraction was immunoblotted using anti-NCLX antibody pre-incubated with or without NCLX blocking peptide.

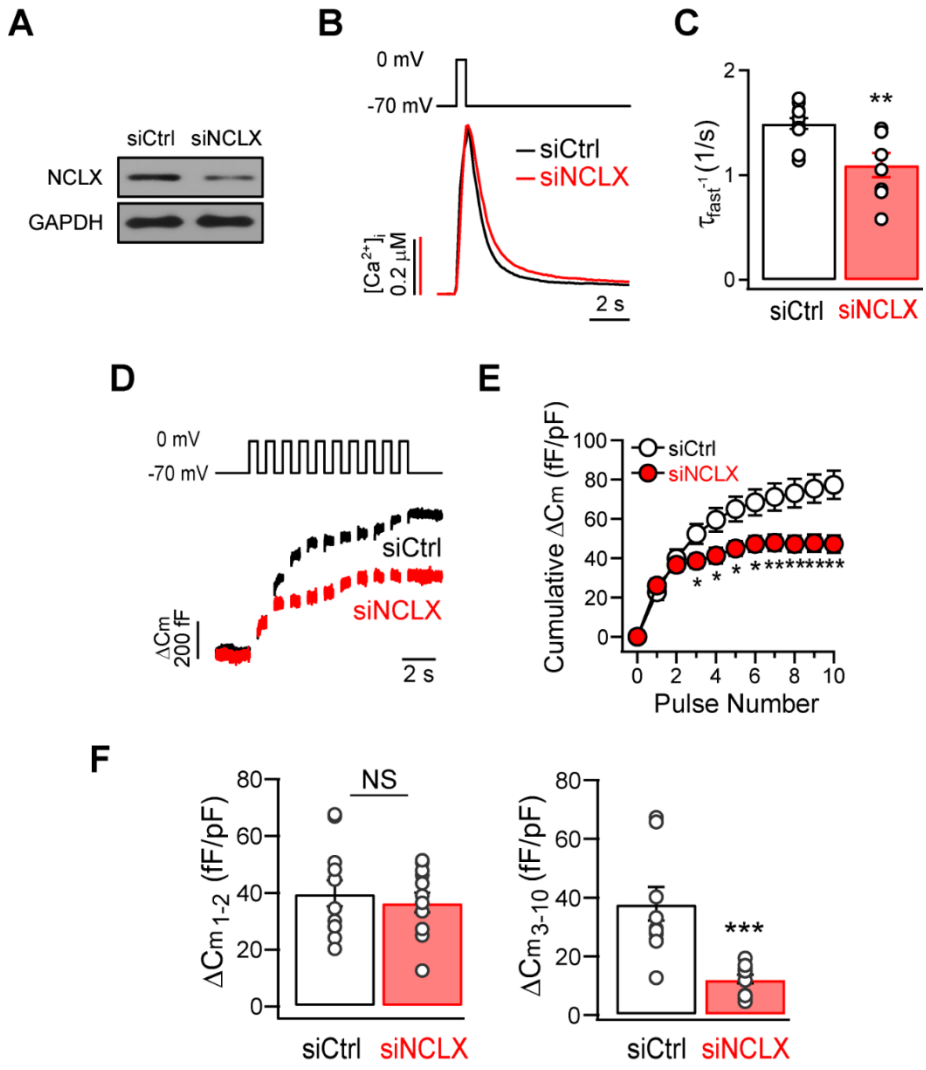

Figure 6. Effect of NCLX knockdown on Ca^{2+} clearance and depolarization-induced exocytosis.

(A) Knockdown of endogenous NCLX in siNCLX-transfected INS-1 cells. Western blot analysis of endogenous NCLX in lysates from INS-1 cells transfected with siControl (siCtrl) or siNCLX. GAPDH was detected as a loading control. Marked reduction of endogenous NCLX expression was found

in siNCLX-transfected INS-1 cells. **(B, C)** The experiments and analyses were the same as Fig. 3. **(B)** Representative Ca^{2+} transients (CaTs) recorded in siCtrl- (black) and siNCLX- (red) transfected cells. **(C)** Mean values for fast decay rate constants (τ_{fast}^{-1}) of CaTs (siCtrl, open bar, *n*=12; siNCLX, red bar, *n*=8). Open circles represent individual values for τ_{fast}^{-1}. ***P*<0.01 compared with siCtrl. **(D)** Experimental protocol for whole-cell capacitance measurement illustrating ten consecutive 500 ms depolarizing pulses from a holding potential of -70 to 0 mV applied at 1 Hz. Representative capacitance traces from INS-1 cells expressing siCtrl or siNCLX. **(E)** Averaged cumulative ΔC_m at individual depolarization number for siCtrl- (open circle, *n*=12) and siNCLX- (red circle, *n*=12) transfected cells. **P*<0.05 and ***P*<0.01 compared with siCtrl. **(F)** Averaged ΔC_m during the first two pulses and the 3-10 pulses. Open circles represent individual values. ****P*<0.001 compared with siCtrl. NS, not significant.

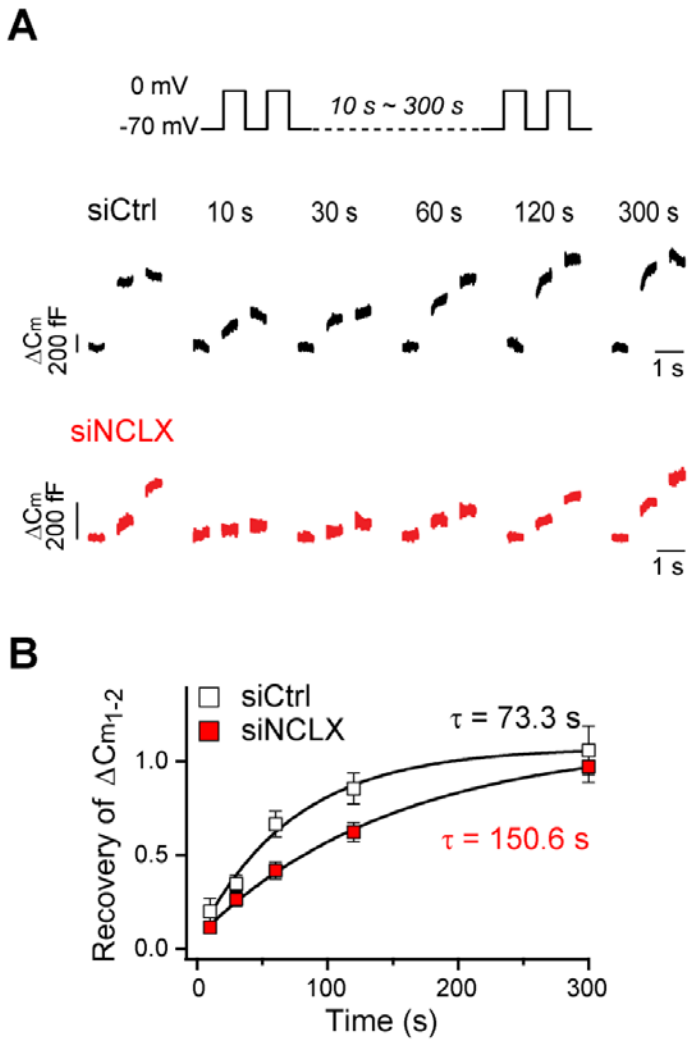

Figure 7. NCLX knockdown delays RRP recovery.

(A) Representative capacitance traces of two consecutive 500 ms pulses with time intervals from 10–300 s in cells expressing siCtrl (black) or siNCLX (red). **(B)** The sum of the capacitance increment by the two pulses ($\Delta C_{m1\text{-}2}$) obtained from siCtrl (open square, *n*=5) and siNCLX (red square, *n*=5) was plotted

against time intervals. The data were fitted with single exponential functions and time constants of recovery (τ) were obtained as indicated.

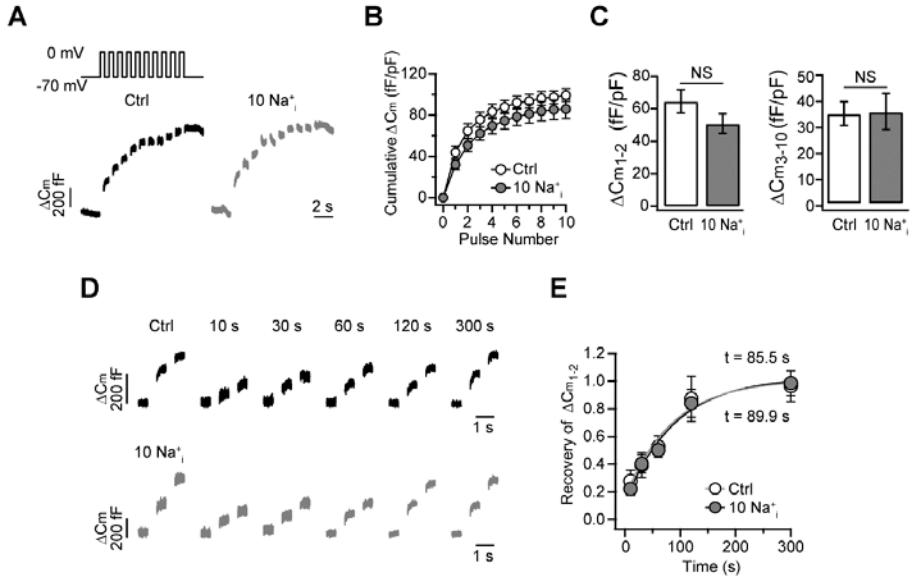

Figure 8. Effect of intracellular Na^+ on depolarization-induced exocytosis.

The experimental protocol and analyses were the same as in Figs. 6D-F and 7. **(A)** Representative capacitance traces from the INS-1 cells in 0 mM Na^+-(Control, Ctrl) and 10 mM Na^+-containing internal solution (10 Na^+_i). **(B, C)** Averaged cumulative ΔC_m and averaged ΔC_m during the 1-2 and 3–10 pulses for Ctrl (open, *n*=12) and 10 Na^+_i conditions (gray, *n*=11). **(D, E)** Averaged recovery of the sum of two ΔC_m with time intervals and time constants of recovery (τ) for Ctrl (*n*=7) and 10 Na^+_i conditons (*n*=8). NS, not significant.

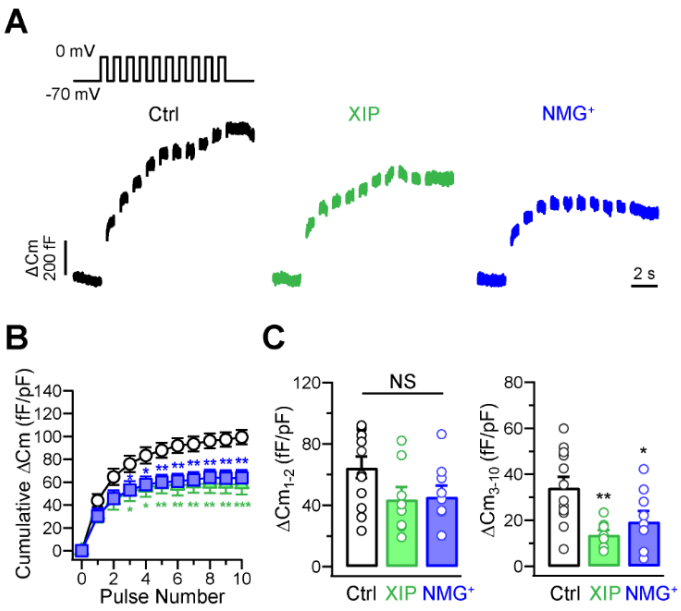

Figure 9. Effect of inhibiting NCX and Na^+ replacement on depolarization-induced exocytosis.

The experimental protocol and analyses were the same as in Fig. 6 (D-F). **(A)** Representative capacitance traces from the INS-1 cells in the absence (open; Control, Ctrl) or presence of XIP (green) in the Na^+-free pipette solution or substitution of external Na^+ with NMG^+ (103 mmol/l $[NMG^+]_o$ + 20 mmol/l $[Na^+]_o$). **(B, C)** Averaged cumulative ΔC_m and averaged ΔC_m during the first and second phase for Ctrl (open, n=12), 10 µmol/l XIP (green, n=8) and NMG^+ substitution (blue, n=9). *p<0.05, **p<0.01 and ***p<0.001 compared with Ctrl.

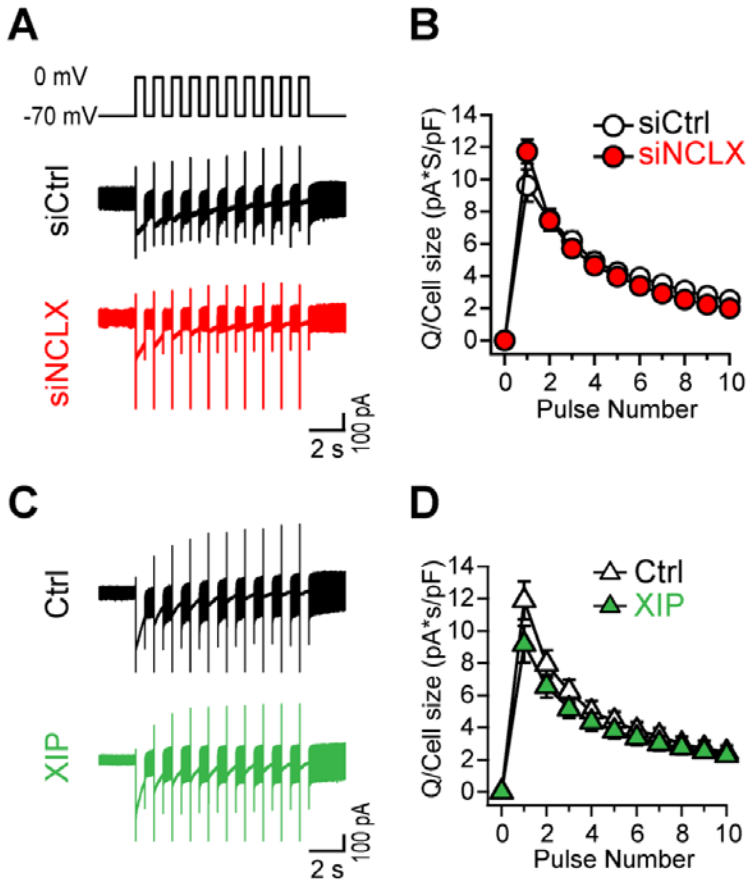

Figure 10. siNCLX or NCX inhibition by XIP does not affect voltage-dependent Ca^{2+} currents.

(A) Representative voltage-dependent Ca^{2+} current traces from the siCtrl- or siNCLX-transfected cells elicited by the same pulses as displayed in Fig.6. **(B)** Averaged current integral at individual depolarization number for the siCtrl- (open circle, n=12) and siNCLX-transfected cells (red circle, n=12). Q is the integral of Ca^{2+} currents and is normalized to cell size. **(C, D)** The same

experiments and analyses as **(A, B)** that the comparison was carried out in the absence (Ctrl; open triangle, n=12) and presence (green triangle, n=8) of 10 µmol/l XIP in Na^+-free pipette solution.

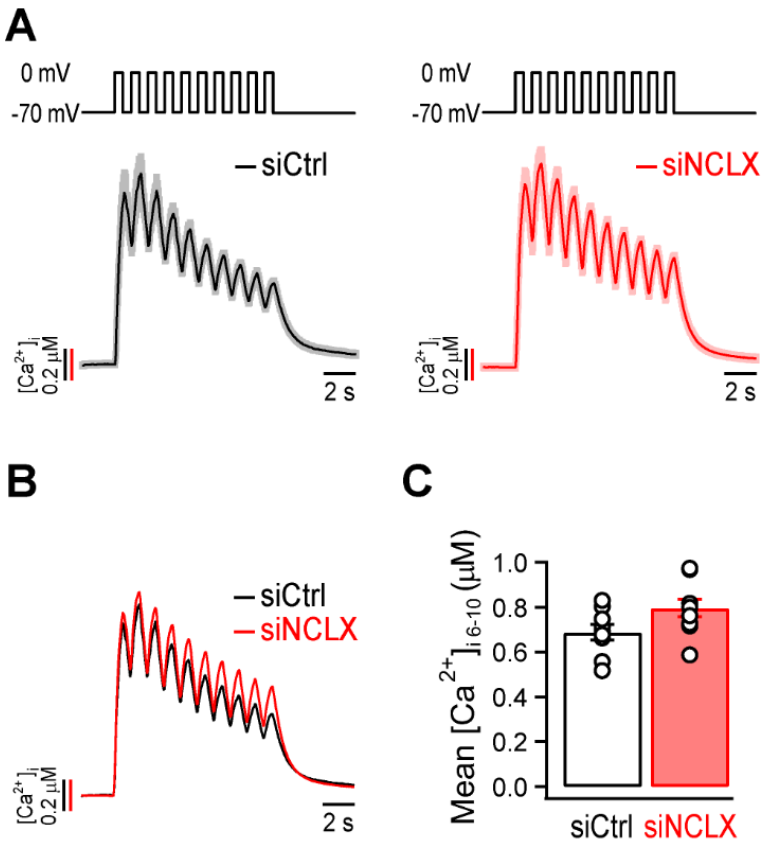

Figure 11. The effect of NCLX knockdown on Ca^{2+} responses to ten depolarizations.

(A) Averaged traces of Ca^{2+} transients elicited by ten depolarization pulses from siCtrl- (left, *n*=9) and siNCLX-transfected cells (right, *n*=11). Standard errors were indicated with pale colors. **(B)** Superimposition of two average traces shown in (A). **(C)** Mean values for averaged $[Ca^{2+}]_i$ between the 6th and 10th pulses of Ca^{2+} transients from siCtrl- (open bar, *n*=9) and siNCLX-transfected cells (red bar, *n*=11) shown in (A). Open circles represent individual values for mean $[Ca^{2+}]_{i\ 6\text{-}10}$. *P*=0.053 compared with siCtrl.

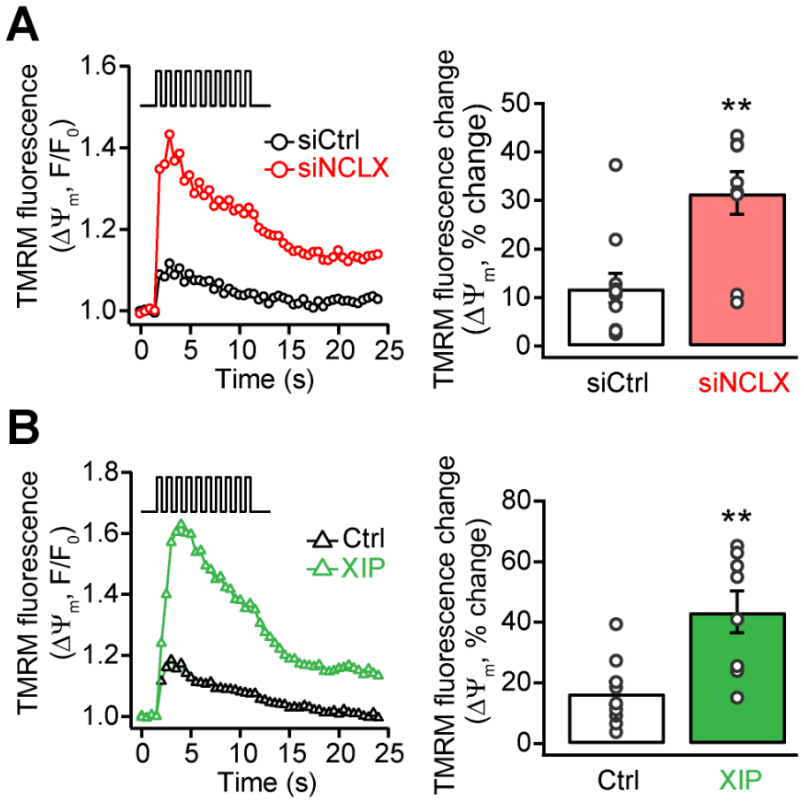

Figure 12. Effect of siNCLX or NCX inhibition by XIP on mitochondrial membrane potential.

(A) Representative TMRM fluorescence traces recorded in siCtrl- and siNCLX-transfected cells, elicited by a train of ten 500 ms depolarizations from -70 to 0 mV (left). Averaged TMRM fluorescence changes as percent increase from initial levels before the depolarizing pulse in cells expressing siCtrl (open circle, n=11) or siNCLX (red circle, n=9) (right). **p<0.01 compared with Ctrl.

(B) The experiments and analyses were the same as in (A), with the exception that the comparison was carried out in the absence (Ctrl; open triangle, n=9)

and presence (green triangle, n=8) of 10 μmol/l XIP in the Na^+-free pipette solution. **p<0.01 compared with Ctrl.

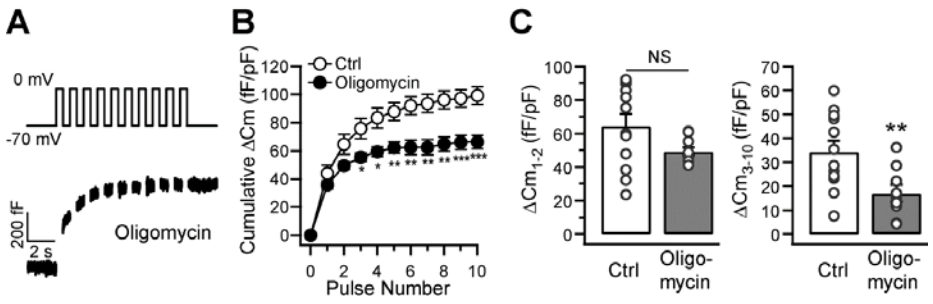

Figure 13. Effect of oligomycin on depolarization-induced exocytosis.

(A-C) The experimental protocol and analyses were the same as in Fig. 6 (D-F), with the exception that the comparison was carried out in the absence (Ctrl; open circle, n=12) or presence (closed circle, n=9) of 2.5 μg/mL oligomycin in Na^+-free internal solution. *p<0.05, **p<0.01 and ***p<0.001 compared with Ctrl.

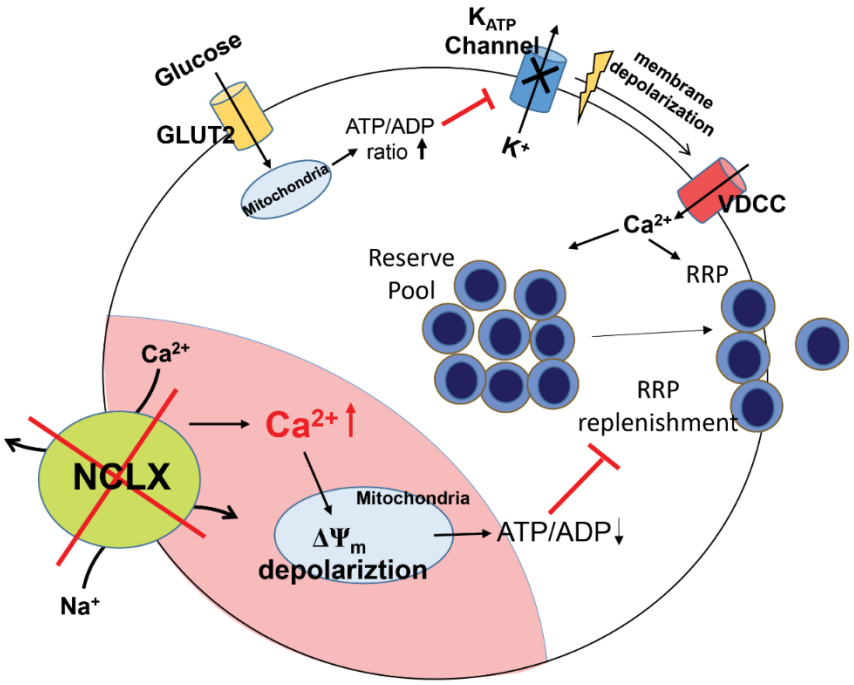

Figure 14. Schematic diagram for the role of NCLX in the exocytosis of pancreatic β-cell.

The activity of surface NCLX may regulate local Ca^{2+} to optimize mitochondrial local metabolic control and thus contributes to vesicle recruitment for the normal secretory function in pancreatic β-cells.

DISCUSSION

In the present study, I showed that Na^+-dependent Ca^{2+} transport across the plasma membrane in pancreatic β-cells is mediated by NCLX as well as NCX. The presence of NCLX in the plasma membrane was confirmed by immunocytochemistry and western blot analysis with cell surface biotinylation. Furthermore, I discovered that normal Ca^{2+} clearance mediated by NCLX and NCX activities is crucial for normal mitochondrial function, which underlies vesicle recruitment, particularly in the sustained phase of exocytosis.

The physiological roles of NCX in β-cells have been investigated in several studies, but the results are controversial. NCX Inhibition with KB-R7943 or shRNA-mediated downregulation of NCX1 enhanced glucose-induced Ca^{2+} responses, depolarization-induced exocytosis and insulin secretion in mouse and human β-cells (Hamming et al., 2010), whereas knockdown of NCX1 with antisense oligonucleotides in rat β-cells significantly inhibited Ca^{2+} increases induced by high K^+, sulfonylurea or high glucose (Van Eylen et al., 1998). Despite these different results, both studies assumed that NCX contributes to insulin secretion via regulating cytosolic Ca^{2+}. Increased or decreased cytosolic Ca^{2+} by NCX inhibition, resulting from inhibiting the forward or reverse mode

of NCX, was considered to be responsible for the increase or decrease in insulin secretion.

The role of mNCX in pancreatic β-cells has been of a great interest because this Ca^{2+} transporter controls intramitochondrial Ca^{2+} as well as cytosolic Ca^{2+}. In previous studies, CGP-37157 was used as a specific inhibitor for mNCX, but there are conflicting results regarding the effect of CGP-37157 on GSIS. CGP-37157 enhanced GSIS in INS-1 cells or rat islets, whereas CGP-37157 at the same concentration used by Lee *et al*. (2003) diminished GSIS in mouse islets (Luciani et al., 2007). Considering that CGP-37157 also inhibits voltage-gated Ca^{2+} influx (Luciani et al., 2007), the results obtained using CGP-37157 may require re-interpretation. Since NCLX was identified as a mNCX (Palty et al., 2010), the role of mNCX in pancreatic β-cell functions has been investigated actively using siNCLX or a dominant negative construct of NCLX (Nita et al., 2012; Nita et al., 2015). The results of these studies suggest that mNCX controls the rate and amplitude of cytosolic Ca^{2+} concentration induced by depolarization or high glucose, and thus, regulating insulin secretion. In these studies, however, the possibility that NCLX is also operating on the plasma membrane and that the knockdown of NCLX affects both mitochondrial and plasmalemmal NCLX has not been considered. For example, mitochondrial

Ca^{2+} increase in response to 20 mM glucose was potentiated by siNCLX (Nita et al., 2012), and this result was interpreted as an indication of the role of mNCX in mitochondrial Ca^{2+} regulation. However, in the light of the knowledge that NCLX also acts as plasmalemmal Na^+/Ca^{2+} exchanger, inhibition of Ca^{2+} clearance by siNCLX may cause cytosolic Ca^{2+} increase, which in turn contributes to the mitochondrial Ca^{2+} increase.

In fact, the current density of Li^+/Ca^{2+} exchange activity was ~50% of the total Na^+/Ca^{2+} exchange activity in cultured rat skeletal myotubes (Deval et al., 2002), and in rat ventricular myocytes, cell surface NCLX was detected by immunocytochemistry using specific antibodies (Cai and Lytton, 2004). However, the presence and role of NCLX on the plasma membrane of pancreatic β-cells have not been considered. My Ca^{2+} dynamics data obtained from fluorescent Ca^{2+} imaging indicated the presence of Li^+-permeable Na^+/Ca^{2+} exchangers on the plasma membrane in INS-1 cells (Figs. 3 and 4), and I confirmed the expression of NCLX in the plasma membrane through immunochemistry, surface biotinylation and subsequent western blot analysis (Fig. 5B and C). NCLX was originally classified as K^+-dependent Na^+/Ca^{2+} exchanger 6 (NCKX6), but the K^+-dependency of Ca^{2+} transport through this carrier is controversial (Cai and Lytton, 2004; Palty et al., 2004). My study

supports the idea that the NCLX is not K^+-dependent (Fig. 4E and F). Furthermore, to exclude the contribution of mitochondrial NCLX and investigate the role of plasmalemmal NCLX exclusively, I evaluated the effect of mNCX on the depolarization-induced capacitance increase by comparing the results obtained in Na^+-free internal solution and those in 10 mM Na^+-containing internal solution (Fig. 8); no significant differences were observed, suggesting that mNCX did not contribute to the secretory function of β-cells. Under this Na^+-free condition, I also found that inhibition of cytosolic Ca^{2+} clearance by siNCLX, which induced a slight increase in cytosolic Ca^{2+} (Fig. 11), did not lead to the increase in exocytosis, but rather suppressed sustained insulin release in response to repetitive stimulation (Fig. 6). These results imply that cytosolic Ca^{2+} clearance during repetitive stimulation may not have an inhibitory effect on exocytosis, but is required, especially for sustained insulin release. In searching for the underlying mechanisms, I found that depolarization of the mitochondrial membrane potential during repetitive stimulation is significantly accelerated by siNCLX (Fig. 12). Therefore, I propose the possibility that impaired Ca^{2+} clearance by siNCLX may induce impaired mitochondrial function and that impaired ATP production leads to the inhibition of vesicle recruitment or priming reaction required for sustained

exocytosis. All these effects of siNCLX described above are almost identical to the effects of XIP or external Na^+ replacement (Fig. 9 and 12), further supporting the idea that the effects of siNCLX and XIP are attributable to the effects of inhibiting plasmalemmal Na^+/Ca^{2+} exchange activities. My results appeared inconsistent with previous results that NCX1 inhibition augmented depolarization-induced capacitance increase in mouse and human β-cells (Hamming et al., 2010). In addition to the differences in NCX1 inhibition effects, the difference in the control response was also noted. Under control conditions, my results showed two distinctive phases in capacitance increase in response to ten depolarization pulses, whereas other studies showed a monotonic increase. While the reasons for these differences are unclear, it is possible that differences in species or experimental conditions may be involved. To examine such possibilities, future experiments should assess the effect of pNCEx inhibition on depolarization-induced capacitance increase in different species under the same experimental conditions.

Finally, I demonstrated that the effect of inhibiting mitochondrial ATP synthesis using oligomycin on depolarization-induced exocytosis resembled strikingly with the effect of inhibiting plasmalemmal Na^+/Ca^{2+} exchangers (Fig. 13), suggesting that these two processes share a common mechanism. Taken

together, it is suggested that the plasmalemmal Na^+/Ca^{2+} exchange has a crucial role in the regulation of mitochondrial functions and thus, the regulation of sustained insulin release. In this respect, NCLX is as important as NCX. My study gives a new insight on the relationship between cytosolic Ca^{2+} and sustained insulin release, in that sustained insulin release is not simply potentiated by the increase in cytosolic Ca^{2+} level, but proper Ca^{2+} clearance during massive Ca^{2+} influx is critical for optimizing mitochondrial function to supply ATP for vesicle recruitment (Fig. 14).

Capacitance measurements have been widely used to elucidate the cellular mechanism underlying insulin secretion from pancreatic β-cells (Kanno et al., 2004). It is generally accepted that the initial phase of rapid C_m increment reflects exocytosis from a subset of RRP located near Ca^{2+} channels (Barg et al., 2001b), but the mechanisms that underlie sustained exocytosis in response to repetitive depolarization is less clear. It was shown that ADP or DIDS (a Cl^- channel blocker) selectively inhibited sustained exocytosis, suggesting that sustained exocytosis requires ATP-dependent vesicle priming steps (Barg et al., 2001a; Rorsman et al., 2000a). I demonstrated that siNCLX not only inhibited sustained exocytosis in response to repetitive depolarization, but also inhibited the recovery of RRP (Figs. 6 and 7). Inhibition of sustained exocytosis and

recovery of RRP after depletion was also reported in pancreatic β-cells lacking Munc13-1, a presynaptic protein that is essential for synaptic vesicle priming (Kang et al., 2006). These results support the idea that sustained exocytosis in response to repetitive depolarization reflects the continuous recruitment or priming of insulin vesicles.

It is well known that GSIS occurs in a biphasic pattern, consisting of an initial rapid first phase and slow sustained second phase (Curry et al., 1968). The second phase is characteristic of insulin secretion evoked only by fuel secretagogues, which is not observed when high extracellular K^+ and tolbutamide stimulate insulin secretion (Gembal et al., 1992; Rorsman et al., 2000b). Thus, the second phase of insulin secretion has been attributed to RRP refilling through mobilization of granules from a reserve pool, which is ATP-dependent (Eliasson et al., 1997; Henquin et al., 2002). In this respect, sustained exocytosis monitored by C_m increment in response to repetitive depolarization may reflect the common mechanism involved in the second phase of GSIS (Barg et al., 2002). In support of such an idea, the second phase of GSIS was abolished in Munc13-1 knock-out mice where sustained insulin release upon prolonged stimulation was suppressed (Kang et al., 2006). However, oversimplification should be avoided.

In conclusion, Ca^{2+} clearance mediated by NCLX and NCX regulates local Ca^{2+} to optimize mitochondrial function, thereby contributing to vesicle recruitment for normal secretory function in pancreatic β-cells.

REFERENCES

Ashcroft, F.M., Proks, P., Smith, P.A., Ämmälä, C., Bokvist, K., and Rorsman, P. (1994). Stimulus–secretion coupling in pancreatic β cells. J. Cell. Biochem. *55*, 54-65.

Ashcroft, F.M., and Rorsman, P. (1989). Electrophysiology of the pancreatic β-cell. Prog. Biophys. Mol. Biol. *54*, 87-143.

Barg, S., Eliasson, L., Renström, E., and Rorsman, P. (2002). A subset of 50 secretory granules in close contact with L-type Ca^{2+} channels accounts for first-phase insulin secretion in mouse β-cells. Diabetes *51* S74-S82.

Barg, S., Huang, P., Eliasson, L., Nelson, D.J., Obermüller, S., Rorsman, P., Thévenod, F., and Renström, E. (2001a). Priming of insulin granules for exocytosis by granular Cl^- uptake and acidification. J. Cell Sci. *114*, 2145-2154.

Barg, S., Ma, X., Eliasson, L., Galvanovskis, J., Gopel, S.O., Obermuller, S., Platzer, J., Renstrom, E., Trus, M., Atlas, D., et al. (2001b). Fast exocytosis with few Ca^{2+} channels in insulin-secreting mouse pancreatic B cells. Biophys. J. *81*, 3308-3323.

Bernardi, P. (1999). Mitochondrial transport of cations: channels, exchangers, and permeability transition. Physiol. Rev. *79*, 1127-1155.

Berridge, M.J., Bootman, M.D., and Roderick, H.L. (2003). Calcium signalling: dynamics, homeostasis and remodelling. Nat. Rev. Mol. Cell Biol. *4*, 517-529.

Berridge, M.J., Lipp, P., and Bootman, M.D. (2000). The versatility and universality of calcium signalling. Nat. Rev. Mol. Cell Biol. *1*, 11-21.

Cai, X., and Lytton, J. (2004). Molecular cloning of a sixth member of the K^+-dependent Na^+/Ca^{2+} exchanger gene family, NCKX6. J. Biol. Chem. *279*, 5867-5876.

Chen, L., Koh, D.S., and Hille, B. (2003). Dynamics of calcium clearance in mouse pancreatic beta-cells. Diabetes *52*, 1723-1731.

Crompton, M., and Heid, I. (1978). The cycling of calcium, sodium, and protons across the inner membrane of cardiac mitochondria. Eur. J. Biochem. *91*, 599-608.

Curry, D.L., Bennett, L., and Grodsky, G.M. (1968). Dynamics of insulin secretion by the perfused rat pancreas. Endocrinology *83*, 572-584.

Deval, E., Raymond, G., and Cognard, C. (2002). Na^+–Ca^{2+} exchange activity in rat skeletal myotubes: effect of lithium ions. Cell Calcium *31*, 37-44.

Eliasson, L., Renström, E., Ding, W.-G., Proks, P., and Rorsman, P. (1997). Rapid ATP-dependent priming of secretory granules precedes Ca^{2+}-induced exocytosis in mouse pancreatic B-cells. The Journal of Physiology *503*, 399-

412.

Gall, D., Gromada, J., Susa, I., Rorsman, P., Herchuelz, A., and Bokvist, K. (1999). Significance of Na/Ca exchange for Ca^{2+} buffering and electrical activity in mouse pancreatic β-cells. Biophys. J. *76*, 2018-2028.

Gembal, M., Gilon, P., and Henquin, J.C. (1992). Evidence that glucose can control insulin release independently from its action on ATP-sensitive K^{+} channels in mouse B cells. J. Clin. Invest. *89*, 1288-1295.

Hamming, K.S., Riedel, M.J., Soliman, D., Matemisz, L.C., Webster, N.J., Searle, G.J., MacDonald, P.E., and Light, P.E. (2008). Splice variant-dependent regulation of β-cell sodium-calcium exchange by acyl-coenzyme As. Mol. Endocrinol. *22*, 2293-2306.

Hamming, K.S., Soliman, D., Webster, N.J., Searle, G.J., Matemisz, L.C., Liknes, D.A., Dai, X.Q., Pulinilkunnil, T., Riedel, M.J., Dyck, J.R., et al. (2010). Inhibition of β-cell sodium-calcium exchange enhances glucose-dependent elevations in cytoplasmic calcium and insulin secretion. Diabetes *59*, 1686-1693.

Henquin, J.-C., Ishiyama, N., Nenquin, M., Ravier, M.A., and Jonas, J.-C. (2002). Signals and pools underlying biphasic insulin secretion. Diabetes *51*, S60-S67.

Herchuelz, A., Diaz-Horta, O., and Van Eylen, F. (2002). Na/Ca exchange and Ca^{2+} homeostasis in the pancreatic beta-cell. Diabetes Metab. *28*, 3S54-60; discussion 53S108-112.

Herchuelz, A., Kamagate, A., Ximenes, H., and Van Eylen, F. (2007). Role of Na/Ca exchange and the plasma membrane Ca^{2+}–ATPase in β cell function and death. Ann. N. Y. Acad. Sci. *1099*, 456-467.

Hernández-SanMiguel, E., Vay, L., Santo-Domingo, J., Lobatón, C.D., Moreno, A., Montero, M., and Alvarez, J. (2006). The mitochondrial Na^{+}/Ca^{2+} exchanger plays a key role in the control of cytosolic Ca^{2+} oscillations. Cell Calcium *40*, 53-61.

Hughes, E., Lee, A.K., and Tse, A. (2006). Dominant role of sarcoendoplasmic reticulum Ca^{2+}-ATPase pump in Ca^{2+} homeostasis and exocytosis in rat pancreatic β-cells. Endocrinology *147*, 1396-1407.

Kamagate, A., Herchuelz, A., and Van Eylen, F. (2002). Plasma membrane Ca^{2+}-ATPase overexpression reduces Ca^{2+} oscillations and increases insulin release induced by glucose in insulin-secreting BRIN-BD11 cells. Diabetes *51*, 2773-2788.

Kang, L., He, Z., Xu, P., Fan, J., Betz, A., Brose, N., and Xu, T. (2006). Munc13-1 is required for the sustained release of insulin from pancreatic β cells. Cell Metab. *3*, 463-468.

Kanno, T., Ma, X., Barg, S., Eliasson, L., Galvanovskis, J., Gopel, S., Larsson, M., Renstrom, E., and Rorsman, P. (2004). Large dense-core vesicle exocytosis in pancreatic β-cells monitored by capacitance measurements. Methods *33*, 302-311.

Lee, B., Miles, P.D., Vargas, L., Luan, P., Glasco, S., Kushnareva, Y., Kornbrust, E.S., Grako, K.A., Wollheim, C.B., Maechler, P., et al. (2003). Inhibition of mitochondrial Na^+-Ca^{2+} exchanger increases mitochondrial metabolism and potentiates glucose-stimulated insulin secretion in rat pancreatic islets. Diabetes *52*, 965-973.

Leibiger, I.B., Leibiger, B., and Berggren, P.-O. (2008). Insulin signaling in the pancreatic β-cell. Annu. Rev. Nutr. *28*, 233-251.

Lim, A., Park, S.-H., Sohn, J.-W., Jeon, J.-H., Park, J.-H., Song, D.-K., Lee, S.-H., and Ho, W.-K. (2009). Glucose deprivation regulates K_{ATP} channel trafficking via AMP-activated protein kinase in pancreatic β-cells. Diabetes *58*, 2813-2819.

Luciani, D.S., Ao, P., Hu, X., Warnock, G.L., and Johnson, J.D. (2007). Voltage-gated Ca^{2+} influx and insulin secretion in human and mouse β-cells are impaired by the mitochondrial Na^+/Ca^{2+} exchange inhibitor CGP-37157. Eur. J. Pharmacol. *576*, 18-25.

Lytton, J. (2007). Na^+/Ca^{2+} exchangers: three mammalian gene families control

Ca^{2+} transport. Biochem. J. *406*, 365-382.

MacDonald, P.E., and Rorsman, P. (2006). Oscillations, intercellular coupling, and insulin secretion in pancreatic β cells. PLoS Biol. *4*, e49.

Nita, II, Hershfinkel, M., Fishman, D., Ozeri, E., Rutter, G.A., Sensi, S.L., Khananshvili, D., Lewis, E.C., and Sekler, I. (2012). The mitochondrial Na^+/Ca^{2+} exchanger upregulates glucose dependent Ca^{2+} signalling linked to insulin secretion. PLoS One *7*, e46649.

Nita, I.I., Hershfinkel, M., Lewis, E.C., and Sekler, I. (2015). A crosstalk between Na^+ channels, Na^+/K^+ pump and mitochondrial Na^+ transporters controls glucose-dependent cytosolic and mitochondrial Na^+ signals. Cell Calcium *57*, 69-75.

Palty, R., Ohana, E., Hershfinkel, M., Volokita, M., Elgazar, V., Beharier, O., Silverman, W.F., Argaman, M., and Sekler, I. (2004). Lithium-calcium exchange is mediated by a distinct potassium-independent sodium-calcium exchanger. J. Biol. Chem. *279*, 25234-25240.

Palty, R., Silverman, W.F., Hershfinkel, M., Caporale, T., Sensi, S.L., Parnis, J., Nolte, C., Fishman, D., Shoshan-Barmatz, V., Herrmann, S., et al. (2010). NCLX is an essential component of mitochondrial Na^+/Ca^{2+} exchange. Proc. Natl. Acad. Sci. U. S. A. *107*, 436-441.

Park, S.-H., Ryu, S.-Y., Yu, W.-J., Han, Y.E., Ji, Y.-S., Oh, K., Sohn, J.-W., Lim, A., Jeon, J.-P., Lee, H., et al. (2013). Leptin promotes K_{ATP} channel trafficking by AMPK signaling in pancreatic β-cells. Proc. Natl. Acad. Sci. U. S. A. *110*, 12673-12678.

Rorsman, P., Eliasson, L., Renström, E., Gromada, J., Barg, S., and Göpel, S. (2000a). The cell physiology of biphasic insulin secretion. News Physiol. Sci. *15*, 72-77.

Rorsman, P., Eliasson, L., Renstrom, E., Gromada, J., Barg, S., and Gopel, S. (2000b). The cell physiology of biphasic insulin secretion. News Physiol. Sci. *15*, 72-77.

Rorsman, P., and Renstrom, E. (2003). Insulin granule dynamics in pancreatic beta cells. Diabetologia *46*, 1029-1045.

Stutzmann, G.E., and Mattson, M.P. (2011). Endoplasmic Reticulum Ca2+ Handling in Excitable Cells in Health and Disease. Pharmacol. Rev. *63*, 700-727.

Van Eylen, F., Lebeau, C., Albuquerque-Silva, J., and Herchuelz, A. (1998). Contribution of Na/Ca exchange to Ca^{2+} outflow and entry in the rat pancreatic β-cell: studies with antisense oligonucleotides. Diabetes *47*, 1873-1880.

Van Eylen, F., Svoboda, M., and Herchuelz, A. (1997). Identification,

expression pattern and potential activity of Na/Ca exchanger isoforms in rat pancreatic B-cells. Cell Calcium *21*, 185-193.

Voronina, S.G., Barrow, S.L., Gerasimenko, O.V., Petersen, O.H., and Tepikin, A.V. (2004). Effects of secretagogues and bile acids on mitochondrial membrane potential of pancreatic acinar cells: comparison of different modes of evaluating $\Delta\Psi_m$. J. Biol. Chem. *279*, 27327-27338.

Wiederkehr, A., and Wollheim, C.B. (2008). Impact of mitochondrial calcium on the coupling of metabolism to insulin secretion in the pancreatic β-cell. Cell Calcium *44*, 64-76.

ABSTRACT in KOREAN

췌장 베타세포에서의 인슐린 분비에 세포내 칼슘이 중요한 역할을 함은

은 주지의 사실이다. 포도당 농도 증가에 의한 ATP 민감성 포타슘 통로의 억제가 세포막을 저분극 시키고, 그로 인해 활성화되는 전압의존성 칼슘 통로를 통한 칼슘 유입이 인슐린 과립의 분비를 유발시킴은 여러 연구를 통해 증명되었다. 그러나, 세포내 칼슘을 조절하는 다른 기전들이 인슐린 분비에 어떠한 영향을 미치는가에 대해서는 잘 알려져 있지 않다.

소디움/칼슘 교환기전은 양방향 칼슘 수송체로서 세포내외의 소디움과 칼슘의 농도경사와 막전압에 따라 세포막을 통해 칼슘을 유입시키거나 칼슘을 제거할 수 있을 뿐 아니라, 미토콘드리아의 내막에도 존재하여 미토콘드리아 내 칼슘 농도 조절과 동시에 세포내 칼슘 조절에도 기여함으로써, 이 교환기전은 췌장 베타 세포 내 칼슘 조절에서 중요한 역할을 담당한다. 이 교환기전의 분자적 결정인자와 인슐린 분비에서의 역할에 대해서는 더 많은 연구가 필요하다.

본 논문에서는, 최근에 미토콘드리아의 소디움/칼슘

교환기전으로 밝혀진, 리튬 투과성 소디움/칼슘 교환기가 세포막의 소디움/칼슘 교환기처럼, 쥐의 인슐린종 세포주의 세포막에서 소디움과 칼슘을 교환하는 역할을 한다는 사실을 새롭게 규명했다. 리튬 투과성 소디움/칼슘 교환기가 미토콘드리아 뿐만 아니라, 세포막에서도 발현하는 것을 면역세포화학기법과 세포 표면 바이오티닐레이션 실험을 통해 확인하였다. 또한, 연속적인 저분극 자극에 의해 유도되는 capacitance (C_m)의 증가를 측정함으로써, 세포 분비 (exocytosis)에 대한 리튬 투과성 소디움/칼슘 교환기와 소디움/칼슘 교환기의 역할에 대해서도 살펴보았다. RNA 간섭에 의한 리튬 투과성 소디움/칼슘 교환기의 특이적 억제 또는 소디움/칼슘 교환 억제 펩타이드 (XIP)에 의한 소디움/칼슘 교환기의 억제는, ATP에 의존적인 분비 과립의 동원 (vesicle recruitment)에 의해 발생하는 세포분비(exocytosis)를 현저히 억제시켰다. ATP 합성 효소 저해제 (oligomycin) 를 처리했을 때에도 위와 같은 억제 효과가 나타났다. 세포막에 있는 이 두 소디움/칼슘 교환기가 억제 됐을 때, 미토콘드리아 기능이 손상되는 것을 미토콘드리아 막전압 측정을 통해 알 수 있었다. 한편, 세포 내 소디움을 제거하여, 미토콘드리아에서 발현하는 소디움/칼슘교환기를 억제했을 경우, 저분극에 의한 세포분비에

아무런 영향이 없는 것을 관찰하였다. 위의 실험 결과들을 통해, 본 논문에서는, 췌장 베타세포에서 NCX 뿐만 아니라 NCLX 또한 세포막에서 발현되고, 이 교환 기전에 의한 칼슘 제거 기전이 미토콘드리아 기능을 최적화하는데 필수적이고, 이를 통해 지속적인 인슐린 분비에 필요한 분비 과립 동원에 기여함을 시사한다.

중심 단어: 췌장 베타 세포, 칼슘 수송, 소디움/칼슘 교환기전, 엑소사이토시스, Capacitance

학번 : 2009-30617